ORGANOMETALLICS

Article

Cite This: Organometallics XXXX, XXX, XXX-XXX

pubs.acs.org/Organometallics

C(sp^2)−C(sp^2) Reductive Elimination from Well-Defined Diarylgold(III) Complexes

Kai Kang,[†] Shuanshuan Liu,[‡] Ting Xu,[§] Decai Wang,[‡] Xuebing Leng,[†] Ruopeng Bai,[§] Yu Lan,*[,§] and Qilong Shen*[,†]

[†]Key Laboratory of Organofluorine Chemistry, Shanghai Institute of Organic Chemistry, University of Chinese Academy of Sciences, Chinese Academy of Sciences, 345 Lingling Road, Shanghai 200032, People's Republic of China

[‡]Biotechnology and Pharmaceutical Engineering, Nanjing Tech University, Nanjing, Jiangsu Province 210009, People's Republic of China

[§]School of Chemistry and Chemical Engineering, Chongqing University, Chongqing 400030, People's Republic of China

Supporting Information

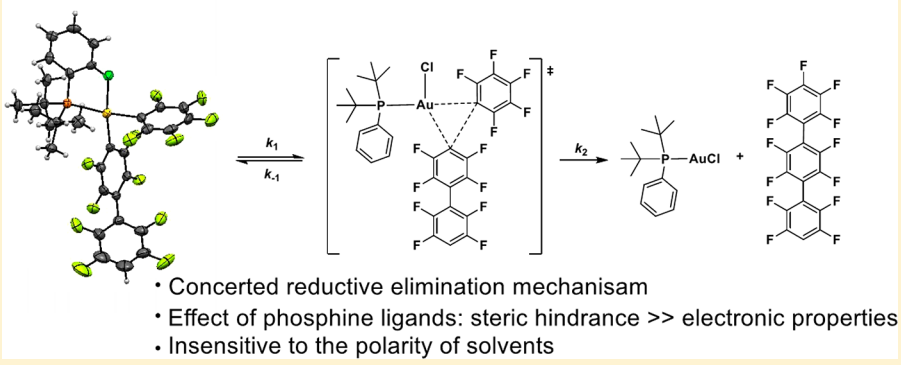

ABSTRACT: A series of well-defined phosphine-ligated diarylgold(III) complexes *cis*-[Au(L)(Ar$_F$)(Ar′)(Cl)] were prepared, and detailed kinetics of the C(sp^2)−C(sp^2) reductive elimination from these complexes were studied. The mechanism of the reductive elimination from the complexes *cis*-[Au(L)(Ar$_F$)(Ar′)(Cl)] was further studied by theoretical calculations. The combination of experimental and theoretical results suggests that the biaryl reductive elimination from organogold(III) complexes *cis*-[Au(L)(Ar$_F$)(Ar′)(Cl)] proceeds through a concerted biaryl-forming pathway from the four-coordinated Au(III) metal center. These studies also disclose that the steric hindrance of the phosphine ligands plays a major role in promoting the biaryl-forming reductive elimination from diarylgold(III) complexes *cis*-[Au(L)(Ar$_F$)(Ar′)(Cl)], while electronic properties of these ligands have a much smaller effect. Futhermore, it was found that the complexes with more weakly electron withdrawing aryl ligands undergo reductive elimination more quickly and the elimination rate is not sensitive to the polarity of the solvents.

INTRODUCTION

Reductive elimination that forms new C−H, C−C, or C−X bonds from two covalent ligands at a transition-metal center is generally considered as a key product-forming elementary reaction in homogeneously catalyzed organic reactions and metal-mediated stoichiometric transformations.[1−3] Over the past 40 years, extensive studies on the reductive elimination of biaryls from square-planar d^8 metal centers such as nickel(II),[4] palladium(II),[5] and platinum(II)[6] have been conducted, and it is well-established that the rates of the reductive elimination reactions are dramatically affected by the steric hindrance and electronic effects of both the ancillary ligands and reactive ligands. These fundamental mechanistic insights have, in turn, enabled the development of high-performance catalytic cross-coupling reactions.[1]

Recently, gold-catalyzed cross-coupling reactions through Au^I/Au^{III} redox cycles have emerged as a new and complementary tool for the construction of carbon−carbon bonds.[7,8] However, unlike other d^8 transition-metal catalysts, fundamental studies on reductive elimination from analogous square-planar d^8 Au(III) centers lag far behind,[9] even though the seminal mechanistic studies on C(sp^3)−C(sp^3) reductive elimination from well-defined trialkylgold(III) complexes by Kochi and co-workers[10] date back to the early 1970s. Only recently, organogold(III) complexes that are able to undergo reductive elimination to form C(sp^2)−C(sp^2),[11] C(sp^2)−N,[12] C(sp^3)−X, and C(sp^2)−X (X = halogen)[13] bonds were identified and the underlying factors that facilitate the reductive elimination started to be uncovered. More specifically, studies on biaryl-forming reductive elimination from organogold(III) complexes remain rather limited. In 1991, Vicente and co-workers reported that, in the presence of PPh$_3$ or a combination of PPh$_3$/NaClO$_4$, the complexes [Au(Ar′)(Ar)-

Received: August 1, 2017

DOI: 10.1021/acs.organomet.7b00588
Organometallics XXXX, XXX, XXX−XXX

(Cl)] underwent facile biaryl reductive elimination at room temperature.[11a] The addition of 2 equiv of PPh_3 did not inhibit the reaction. On the basis of these observations, a concerted $C(sp^2)-C(sp^2)$ reductive elimination mechanism from a four-coordinated gold(III) complex was proposed. A similar example of a $C(sp^2)-C(sp^3)$ mechanism was also reported by this group.[11b] In 2014, Nevado and co-workers showed that the diarylgold(III) complex *cis*-[Au(PPh_3)(C_6F_5)$_2$(Cl)] was rather stable and forcing conditions (150 °C) were required to promote the biaryl reductive elimination.[11c] Likewise, You and co-workers demonstrated that biaryl reductive elimination from [Au(tpy)(Ph)(Br)] (tpy = 2-*o*-tolylpyridine) in ^{t}BuOH occurred smoothly at 80 °C in 98% yield.[11d] In both cases, the detailed mechanism for the elemental reaction was not studied. Toste and co-workers reported, on the basis of kinetic experiments at −52 °C, that biaryl reductive elimination from the in situ formed diarylgold(III) species *cis*-[Au(Ph_3P)(4-F-C_6H_4)$_2$(Cl)] proceeds through a concerted pathway, while the reaction rate increased significantly from the ionic four-coordinated diarylgold(III) species [*cis*-(Ph_3P)$_2$Au(4-F-C_6H_4)$_2$]$^+$Cl$^-$ which formed upon the addition of excess PPh_3.[11e] This mechanistic rationale was further supported by DFT calculations.[11f] More recently, Lloyd-Jones and co-workers revealed that the rates of the intramolecular biaryl reductive elimination from the putative organogold(III) intermediates were accelerated by electron-donating substituents on the aryl rings, while longer and more flexible tethers between two aryl rings also resulted in faster eliminations.[14] Nevertheless, these studies mainly focused on identifying the appropriate conditions to promote biaryl-forming reductive elimination from the Au(III) complexes or kinetic studies of reductive elimination from the in situ formed Au(III) complexes that were identified by ^{31}P and ^{19}F NMR spectroscopy. Fundamental studies to probe the steric and electronic effects of the ancillary ligand on the biaryl-forming reductive elimination from well-defined organogold(III) complexes remain unexplored.

Thus, studies to understand the relative effects of ligand steric and electronic properties on the rates of the $C(sp^2)-C(sp^2)$ bond-forming reductive elimination from well-defined organogold(III) complexes not only will provide fundamental insights into factors that govern the bond-forming process but also could help to reduce experimental efforts during the development of new transition-metal-catalyzed reactions. In this paper, we report crystallographic, kinetic, and theoretical data that illuminate the steric and electronic factors of the ligands on the $C(sp^2)-C(sp^2)$ bond-forming reductive elimination from a series of well-defined diarylgold(III) complexes *cis*-[Au(L)(Ar_F)(Ar′)(Cl)]. Our studies showed: (1) Biaryl reductive elimination from organogold(III) complexes *cis*-[Au(L)(Ar_F)(Ar′)(Cl)] proceeds through a concerted pathway from the four-coordinate Au(III) metal center. (2) Steric hindrance of the phosphine ligand plays a major role in promoting the biaryl reductive elimination from organogold(III) complexes *cis*-[Au(L)(Ar_F)(Ar′)(Cl)], while electronic properties of these ligands have a much smaller effect. (3) The rates of biaryl reductive elimination from organogold(III) complexes *cis*-[Au(L)(Ar_F)(Ar′)(Cl)] were not sensitive to the polarity of the solvents. (4) Diarylgold(III) complexes with more electron withdrawing aryl ligands undergo reductive elimination more quickly.

RESULTS

Synthesis and Characterization of Phosphine-Ligated Diarylgold(III) Complexes *cis*-[Au(L)(Ar_F)(Ar′)(Cl)] (3a−j).

To study the biaryl reductive elimination from organogold(III) complexes, we were facing a considerable challenge that requires the generation of the organogold(III) complexes with two cis aryl groups. We thus first developed a method for the preparation of these complexes, as summarized in Table 1.

Table 1. Synthesis of Phosphine-Ligated Diarylgold(III) Complexes *cis*-[Au(L)(Ar_F)(Ar′)(Cl)] (3a−j)[a]

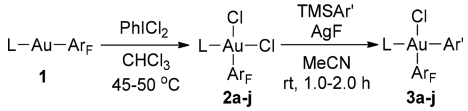

entry	ligand	Ar′	complex, yield (%) 2	3
1	L = PCy_3	C_6F_5	**2a**, 23	**3a**, 56
2	L = $PCy_2{}^t$Bu	C_6F_5	**2b**, 80	**3b**, 54
3	L = $PCy{}^t Bu_2$	C_6F_5	**2c**, 63	**3c**, 62
	L = P(*p*-X-C_6H_4)$^t Bu_2$			
4	X = OMe	C_6F_5	**2d**, 62	**3d**, 54
5	X = Me	C_6F_5	**2e**, 99	**3e**, 68
6	X = H	C_6F_5	**2f**, 70	**3f**, 45
7	X = Cl	C_6F_5	**2g**, 71	**3g**, 53
8	X = CF_3	C_6F_5	**2h**, 47	**3h**, 53
	L = $PPh{}^t Bu_2$			
9	L = $PPh{}^t Bu_2$	*p*-H-C_6F_4		**3i**, 55
10	L = $PPh{}^t Bu_2$	*p*-CF_3-C_6F_4		**3j**, 67

[a] Ar_F =

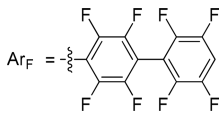

Treatment of [Au(L)(Cl)] with 2,2′,3,3′,5,5′,6,6′-octafluoro-1,1′-biphenyl in the presence of Ag_2O, K_2CO_3, and ^{t}BuCO$_2$H,[15] followed by oxidation of the resulting [Au(L)(Ar_F)] (**1a−h**) with $PhICl_2$[13d,16] in $CHCl_3$ generated the Au(III) complexes *cis*-[Au(L)(Ar_F)Cl$_2$] (**2a−h**) in 23−99% yields. Phosphine-ligated diarylgold(III) complexes **3a−h** were then obtained by reaction of complexes **2a−h** with in situ formed C_6F_5Ag[17] by mixing C_6F_5TMS with AgF in anhydrous acetonitrile. The phosphine-ligated diarylgold(III) complexes were isolated as white solids in 45−68% yields, respectively. Likewise, complexes **3i,j** were synthesized using the corresponding TMS(*p*-H-C_6F_4) or TMS(*p*-CF_3-C_6F_4) as the aryl sources. Complexes **3a−j** were fully characterized by ^{1}H, ^{19}F, and ^{31}P NMR, as well as elemental analysis. The structures of these complexes were determined to have a *cis*-biaryl configuration. The formation of *cis*-diarylgold(III) complexes was mainly due to the stronger trans effect of the phosphine group in comparison to that of the polyfluorinated aryl group and the Au−Cl bond trans to the phosphine ligand is weaker than the Au−Cl bond trans to the polyfluorinated aryl group. For example, the bond distance (2.3222(17) Å) of the Au−Cl bond trans to the phosphine ligand in *cis*-[Au(PPh_3)(Ar_F)(Cl)$_2$] (**2i**) is slightly longer than that of the Au−Cl bond trans to the polyfluorinated aryl group (2.3179(16) Å). Complexes **3a−j** are not air and moisture sensitive. No detectable decomposition was observed after more than 2 months of storage on the shelf

DOI: 10.1021/acs.organomet.7b00588
Organometallics XXXX, XXX, XXX−XXX

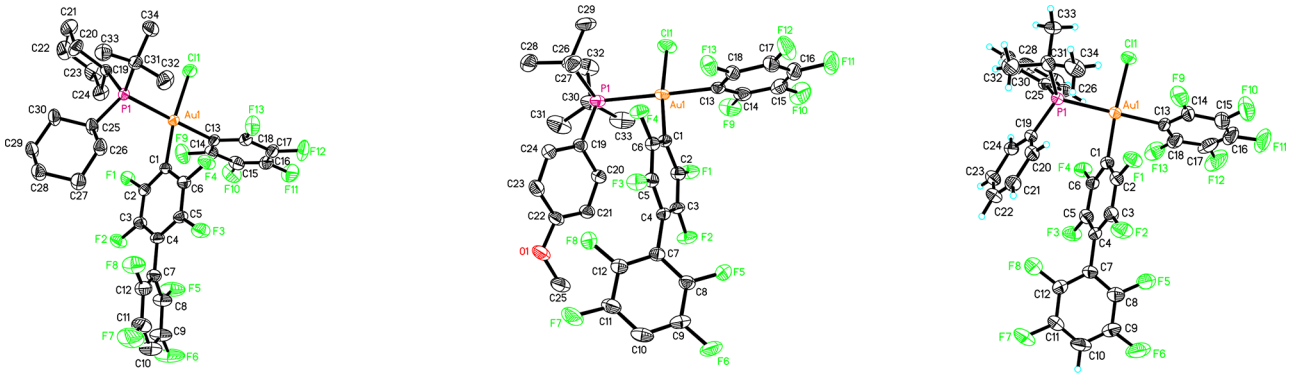

3b 3d 3f

Figure 1. ORTEP diagrams of diarylgold(III) complexes *cis*-[Au(L)(Ar_F)(Ar′)(Cl)] (**3b,d,f**). Ellipsoids are shown at the 50% probability level.

at ambient temperature. These complexes are also stable in solution at room temperature. For example, no decomposition was observed even after 24 h at room temperature when complex **3f** was dissolved in CCl_4, $CDCl_3$, THF, toluene, nitrobenzene, DMF, or CH_3CN, as determined by ^{19}F NMR spectroscopy.

X-ray Structures of Phosphine-Ligated Diarylgold(III) Complexes *cis*-[Au(L)(Ar_F)(Ar′)(Cl)]. Recrystallization of complexes **3a−f,h−j** by slow diffusion of *n*-pentane into a CH_2Cl_2 solution of diarylgold(III) complexes at room temperature gave single crystals that were suitable for analysis by X-ray diffraction. The ORTEP diagrams of phosphine-ligated diarylgold(III) complexes *cis*-[Au(L)(Ar_F)(Ar′)(Cl)] (**3b,d,f**) are shown in Figure 1, and the structures of complexes (**3a,c,e,h−j**) are included in the Supporting Information. Selected bond distances and angles of complexes **3a−f,h−j** are collected in Table 2. In general, the Au−P bond distance in

Table 2. Selected Intramolecular Bond Distances Involving the Non-Hydrogen Atoms of *cis*-[Au(L)(Ar_F)(Ar′)(Cl)] (3a−f,h−j)

	bond distance (Å)			
complex	Au−P	Au−Cl	Au−C(Ar_F)	Au−C(Ar′)
3a	2.3873(14)	2.3291(16)	2.025(5)	2.077(5)
	2.3878(15)	2.3271(15)	2.023(5)	2.062(5)
3b	2.4083(10)	2.3151(11)	2.026(4)	2.059(4)
3c	2.446(8)	2.304(7)	2.04(3)	2.07(3)
	2.426(8)	2.320(7)	2.06(3)	2.11(3)
3d	2.4162(15)	2.3148(13)	2.022(4)	2.068(5)
3e	2.4169(12)	2.3344(11)	2.070(4)	2.046(4)
3f	2.431(2)	2.327(2)	2.049(9)	2.030(9)
3h	2.4155(15)	2.3205(15)	2.048(5)	2.062(5)
3i	2.4385(17)	2.3302(16)	2.058(6)	2.042(6)
3j	2.4326(13)	2.3325(12)	2.053(5)	2.030(5)

complexes **3a−c** (2.3873(10)/2.3878(15), 2.4083(10), and 2.446(8)/2.426(8) Å, respectively) showed an increasing trend because of the increased steric hindrance of the corresponding phosphine ligands (PCy_3, $PCy_2{}^tBu$, and PCy^tBu_2) in these complexes. Complexes **3f,i,j** were ligated by the same phosphine ligand (PhP^tBu_2), wherein the Au−C(Ar′) bond distances in complex **3f** (Ar′ = C_6F_5) and **3j** (Ar′ = *p*-CF_3-C_6F_4) (2.030(5) and 2.030(9) Å, respectively) are slightly shorter than that in complex **3i** (2.042(6) Å, Ar′ = *p*-H-C_6F_4), indicating that the gold−aryl covalent bonds tend to be stronger for aryl ligands that are less electron donating.

As summarized in Table 3, the sums of the four angles around the Au(III) center in these complexes are between 359.98 and 360.71°, demonstrating the square-planar configuration of the gold metal center. The C(Ar_F)−Au−P bond angles in complexes **3a−c** (95.36(15)/93.46(16), 97.06(11), and 99.1(8)/98.9(7)°, respectively) increased with the growth in the steric hindrance of the corresponding phosphine ligand (PCy_3, $PCy_2{}^tBu$, and PCy^tBu_2). To compare the steric hindrance of the phosphine ligands in complexes **3a−f,h−j** quantitatively and more accurately, we use the Cl−Au−C(Ar_F) bond angle to reveal the steric effects of the phosphine ligands in these Au(III) complexes. A smaller Cl−Au−C(Ar_F) bond angle suggests greater steric hindrance of the corresponding ligand. As illustrated in Table 2, the Cl−Au−C(Ar_F) bond angles in complexes **3a−c** (173.89/174.31, 171.27, and 170.5/169.4°, respectively) decrease with an increase in the steric hindrance of the corresponding phosphine ligands of PCy_3, $PCy_2{}^tBu$, and PCy^tBu_2.

C(sp^2)−C(sp^2) Reductive Elimination from *cis*-[Au(L)(Ar_F)(Ar′)(Cl)] (3a−j). No decomposition of *cis*-[Au(PCy_3)(Ar_F)(C_6F_5)(Cl)] (**3a**) was observed when it was heated in $CDCl_3$ at 120 °C for 2 h (Table 4, entry 1). The same reaction conducted at 150 °C for 4 h generated the corresponding reductive elimination product biaryl **4** in quantitative yield (Table 4, entry 2). Thermolysis of *cis*-[Au($PCy_2{}^tBu$)(Ar_F)(C_6F_5)(Cl)] (**3b**) in $CDCl_3$ at 100 °C for 2 h gave biaryl **4** in 23% yield, while heating at 120 °C for 2 h led to 86% conversion of complex **3b** and 82% yield of biaryl **4** (Table 4, entry 3). Reductive elimination from a diarylgold(III) complex ligated with a more sterically hindered phosphine ligand such as PCy^tBu_2 was much faster in comparison to those ligated with PCy_3 or $PCy_2{}^tBu$. Thermolysis of the complex *cis*-[Au(PCy^tBu_2)(Ar_F)(C_6F_5)(Cl)] (**3c**) in $CDCl_3$ at 85 °C occurred with full conversion after 2 h to give the reductive elimination product biaryl **4** in over 95% yield, as determined by ^{19}F NMR spectroscopy (Table 4, entry 4). Likewise, thermolysis of di-*tert*-butyl(aryl)phosphine-ligated organogold(III) complexes *cis*-[Au(P(*p*-X-C_6H_4)$^tBu_2$)(Ar_F)(C_6F_5)(Cl)] (**3d−h**) in $CDCl_3$ at 85 °C generated biaryl **4** in quantitive yields as well (Table 4, entries 5−9). Reductive elimination from a diarylgold(III) complex ligated with P^tBu_3 was much faster. The formation of biaryl **4** was observed in 81% yield after 8 h at room temperature when *cis*-[Au(P^tBu_3)(Ar_F)Cl_2] was treated with a

DOI: 10.1021/acs.organomet.7b00588
Organometallics XXXX, XXX, XXX−XXX

Table 3. Selected Intramolecular Bond Angles Involving the Non-Hydrogen Atoms of *cis*-[Au(L)(Ar_F)(Ar′)(Cl)] (3a−f,h−j)

	bond angle (deg)			
complex	P−Au−C(Ar′)	C(Ar_F)−Au−P	C(Ar_F)−Au−C(Ar′)	Cl−Au−C(Ar_F)
3a	174.21(17)	95.36(15)	86.6(2)	173.89(14)
	172.72(17)	93.46(16)	86.4(2)	174.31(16)
3b	177.09(11)	97.06(11)	85.28(15)	171.27(11)
3c	175.2(7)	99.1(8)	85.7(10)	170.5(8)
	175.4(7)	98.9(7)	85.3(10)	169.4(8)
3d	178.87(14)	94.29(14)	86.45(19)	172.29(14)
3e	174.68(12)	96.03(12)	84.13(16)	169.03(12)
3f	173.4(3)	99.8(3)	85.0(4)	170.0(3)
3h	173.69(17)	96.40(15)	84.8(2)	169.22(16)
3i	176.52(16)	98.71(17)	84.7(2)	170.82(17)
3j	175.79(13)	100.98(14)	82.72(19)	168.35(14)

Table 4. C(sp^2)−C(sp^2) Reductive Elimination Reactions from Complexes 3a−j

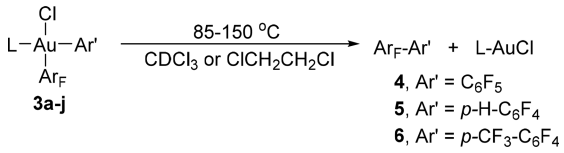

entry	complex **3**	Ar′	solvent	temp (°C)	time (h)	yield of **4** (%)
1	L = PCy_3, **3a**	C_6F_5	$CDCl_3$	120	2	0
2		C_6F_5	$ClCH_2CH_2Cl$	150	4	>95
3	L = $PCy_2{}^tBu$, **3b**	C_6F_5	$CDCl_3$	120	2	82
4	L = $PCy{}^tBu_2$, **3c**	C_6F_5	$CDCl_3$	85	2	>95
	L = $P(C_6H_4$-*p*-X$){}^tBu_2$					
5	X = OMe, **3d**	C_6F_5	$CDCl_3$	85	2	>95
6	X = Me, **3e**	C_6F_5	$CDCl_3$	85	2	>95
7	X = H, **3f**	C_6F_5	$CDCl_3$	85	2	>95
8	X = Cl, **3g**	C_6F_5	$CDCl_3$	85	2	>95
9	X = CF_3, **3h**	C_6F_5	$CDCl_3$	85	2	>95
	L = $PPh{}^tBu_2$					
10	L = $PPh{}^tBu_2$, **3i**	*p*-H-C_6F_4	$CDCl_3$	85	2	>95
11	L = $PPh{}^tBu_2$, **3j**	*p*-CF_3-C_6F_4	$CDCl_3$	85	2	>95

combination of 4.0 equiv of C_6F_5TMS and 2.0 equiv of AgF in MeCN. Presumably, biaryl **4** was generated from in situ formed complex *cis*-[Au($P{}^tBu_3$)(Ar_F)(C_6F_5)(Cl)], which was unstable at room temperature and underwent fast reductive elimination to give **4** in high yield.

Kinetics of the C(sp^2)−C(sp^2) Reductive Elimination from *cis*-[Au(L)(Ar_F)(Ar′)(Cl)] (3c−j). Since the reductive elimination from complexes *cis*-[Au(L)(Ar_F)(Ar′)(Cl)] **3c−j** were clean and high yielding, we studied the kinetics of these reactions in detail. The rates of the C(sp^2)−C(sp^2) reductive elimination reactions from *cis*-[Au(L)(Ar_F)(Ar′)(Cl)] (**3c−j**) were measured by monitoring of the ^{19}F NMR spectroscopy for greater than 3 half-lives. The rate constants were then calculated from plots of the decay of the diarylgold(III) complexes vs time. More specifically, the diarylgold(III) complexes in $CDCl_3$ in a sealed NMR tube were completely immersed in an oil bath maintained at 65 ± 0.1 to 90 ± 0.1 °C and ^{19}F NMR spectra were obtained periodically at room temperature.

Electronic Effects of the Phosphine Ligands on C(sp^2)−C(sp^2) Reductive Elimination from *cis*-[Au(L)(Ar_F)(Ar′)(Cl)] (3d−h). The rates of the C(sp^2)−C(sp^2) reductive elimination reactions from *cis*-[Au(L)(Ar_F)(Ar′)(Cl)] (**3d−h**) were measured at 80 °C, and the results are summarized in Table 5. The disappearance of complexes **3d−h** followed first-order kinetics over more than 3 half-lives. In general, the rate constants for the C(sp^2)−C(sp^2) reductive eliminations from the more electron-poor di-*tert*-butyl(aryl)-phosphine ligated diarylgold(III) complexes were higher than those from the more electron-rich di-*tert*-butyl(aryl)phosphine ligated complexes, while reductive elimination from the complex *cis*-[Au(P(*p*-Me-C_6H_4)$^tBu_2$)(Ar_F)(C_6F_5)(Cl)] (**3e**) is somewhat slower than that from the complex *cis*-[Au(P(*p*-MeO-C_6H_4)$^tBu_2$)(Ar_F)(C_6F_5)(Cl)] (**3d**), although the phosphine ligand P(*p*-OMe-C_6H_4)$^tBu_2$ in complex **3d** is more electron-rich than P(*p*-Me-C_6H_4)$^tBu_2$ in complex **3e**. The order

Table 5. First-Order Kinetics for Thermal Decomposition of Diarylgold(III) Complexes 3d−h at 80 °C

entry	Ar	complex	k_{obs} (10^{-4} s^{-1})	$t_{1/2}$ (s)
1	*p*-MeO-C_6H_4	**3d**	4.13	1676.6
2	*p*-Me-C_6H_4	**3e**	2.62	2647.6
3	C_6H_5	**3f**	4.95	1401.4
4	*p*-Cl-C_6H_4	**3g**	5.29	1309.7
5	*p*-CF_3-C_6H_4	**3h**	6.72	1031.3

DOI: 10.1021/acs.organomet.7b00588
Organometallics XXXX, XXX, XXX−XXX

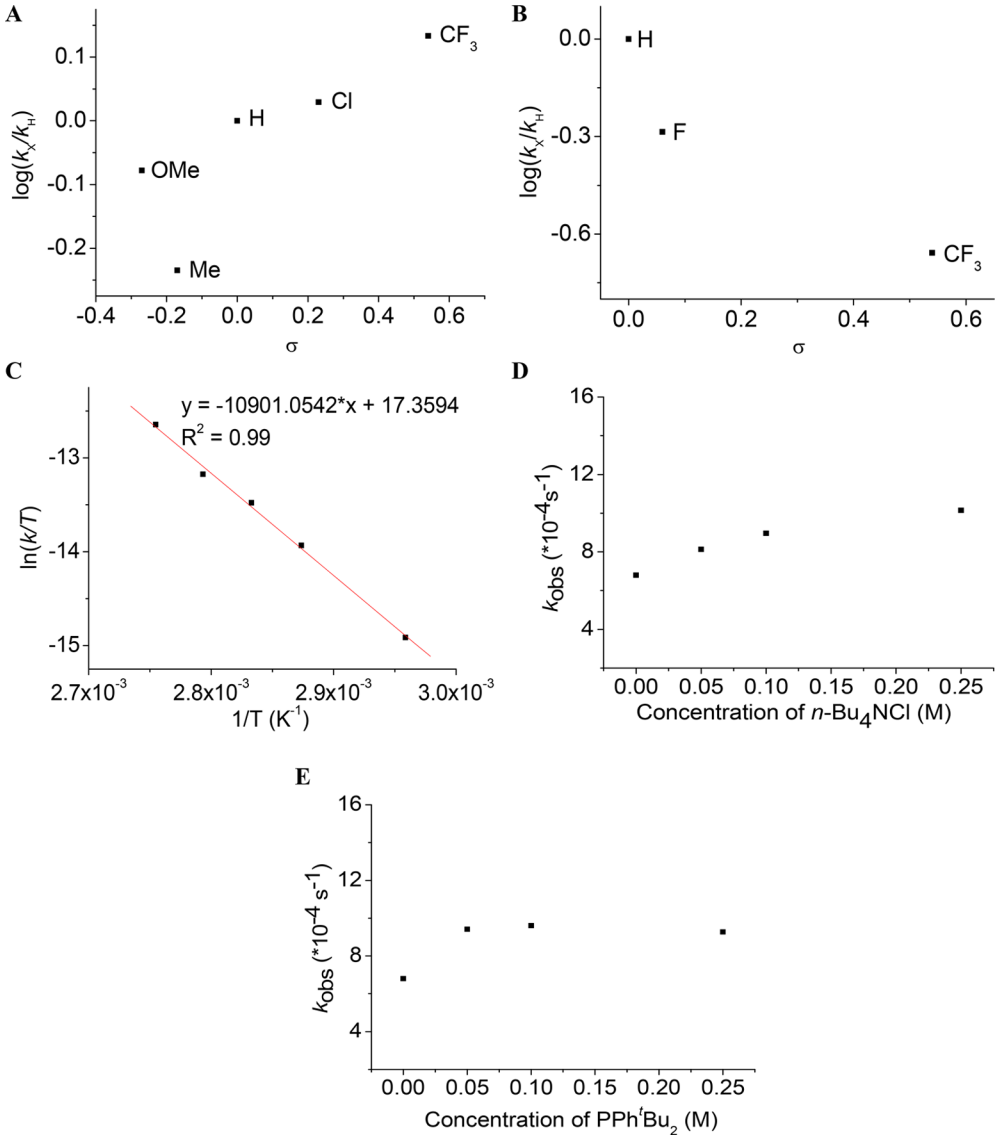

Figure 2. (A) Hammett plot of the rates of the reductive elimination from complexes **3d–h**. (B) Hammett plot of the rates of reductive elimination from complexes **3f,i,j**. (C) Eyring plot for the thermolysis of complex **3f** in $CDCl_3$ over the temperature range 65–90 °C. (D) Effect of added *n*-Bu_4NCl on the rates of thermolysis of complex **3f** at 85 °C in $CDCl_3$. (E) Effect of added PPh^tBu_2 on the rates of thermolysis of complex **3f** at 85 °C in $CDCl_3$.

of these rates for four of the para-substituted di-*tert*-butyl(aryl)phosphine-ligated diarylgold(III) complexes was *p*-CF_3 > *p*-Cl > *p*-H > *p*-MeO. For example, reductive elimination from *cis*-[Au(P(*p*-CF_3-C_6H_4)^{t}Bu$_2$)(Ar_F)(C_6F_5)(Cl)] (**3h**; k_{obs} = 6.72 × 10^{-4} s^{-1}) was roughly 1.5 times faster than that from *cis*-[Au(P(*p*-MeO-C_6H_4)^{t}Bu$_2$)(Ar_F)(C_6F_5)(Cl)] (**3d**; k_{obs} = 4.13 × 10^{-4} s^{-1}). A Hammett plot for the reductive elimination reactions from complexes **3d–h** is shown in Figure 2A. A linear free energy correlation of the rates from complexes **3d,f–h** with the simple σ values derived from benzoic acid acidity was observed. As shown in Figure 2A, a positive value for the parameter ρ was obtained, which indicates that electron-withdrawing substituents at the para position of the aryl group of the phosphine ligands have an accelerating effect on the rate of the C(sp^2)–C(sp^2) reductive elimination.

Electronic Effects of the Aryl Ligands on C(sp^2)–C(sp^2) Reductive Elimination from *cis*-[Au(L)(Ar_F)(Ar′)(Cl)] (3f,i,j). Thermolysis of complexes **3f,i,j** at 85 °C for 2.0 h generated cleanly the corresponding biaryls **4–6** in over 95% yields, respectively (Table 4, entries 7, 10, and 11). The rates of the C(sp^2)–C(sp^2) reductive elimination from these complexes were measured by ^{19}F NMR spectroscopy, and they followed first-order rate laws. As shown in Figure 2B, the C(sp^2)–C(sp^2) reductive elimination from complex **3i** was faster than those of complexes **3f,j**, which demonstrates that electron-donating substituents at the para position of the aryl group that is trans to the phosphine ligand have an accelerating effect on the rates of the carbon–carbon reductive elimination from diarylgold(III) complexes.

Effect of Temperature on C(sp^2)–C(sp^2) Reductive Elimination from *cis*-[Au(PPh^{t}Bu$_2$)(Ar_F)(C_6F_5)(Cl)] (3f). To probe the effect of temperature on the reductive elimination reactions of diarylgold(III) complexes, we studied the kinetics of the C(sp^2)–C(sp^2) reductive elimination from *cis*-[Au(PPh^{t}Bu$_2$)(Ar_F)(C_6F_5)(Cl)] (**3f**) between 65 and 90 °C. It showed a linear dependence of the rates of reductive elimination from complex **3f** with temperatures ranging from 65 to 90 °C, as shown in Figure 2C. The Eyring analysis

DOI: 10.1021/acs.organomet.7b00588
Organometallics XXXX, XXX, XXX–XXX

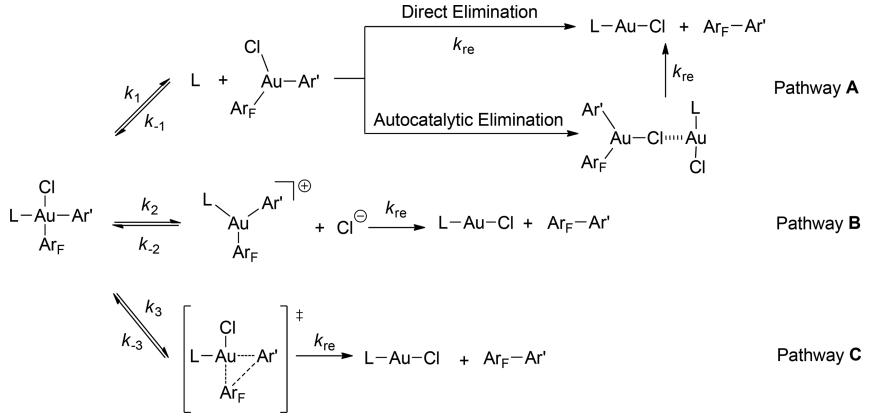

Figure 3. Possible pathways for reductive elimination from diarylgold(III) complexes *cis*-[Au(L)(Ar_F)(Ar′)(Cl)].

revealed activation parameters of $\Delta H^{\ddagger}$ = 21.65 ± 0.77 kcal/mol and $\Delta S^{\ddagger}$ = −12.71 ± 0.73 eu.

Effect of Solvent Polarity on C(sp^2)−C(sp^2) Reductive Elimination from *cis*-[Au(PPh^{t}Bu$_2$)(Ar_F)(C_6F_5)(Cl)] (3f). It is generally known that the rate of reductive elimination from a transition-metal center is greatly affected by the polarity of the reaction medium because of the different relative stabilization effects on the ground and transition states of the transition-metal complexes.[18] To evaluate the effect of solvent polarity on the C(sp^2)−C(sp^2) reductive elimination of the phosphine-ligated diarylgold(III) complexes, we studied the reductive elimination of the complex *cis*-[Au(PPh^{t}Bu$_2$)(Ar_F)(C_6F_5)(Cl)] (**3f**) in different solvents. It was found that heating of complex **3f** in CCl_4, $CDCl_3$, and nitrobenzene led to full conversion after 8 h at 85 °C to give the corresponding biaryl product **4** in almost quantitative yields. Thermolysis of complex **3f** in toluene, DMF, and CH_3CN occurred with full conversion after 8 h to give the corresponding biaryl compound **4** in 97%, 99%, and 99% yields, respectively. To determine the effect of the solvent polarity more precisely, we conducted two sets of parallel experiments to measure the rates of the C(sp^2)−C(sp^2) reductive elimination from *cis*-[Au(PPh^{t}Bu$_2$)(Ar_F)(C_6F_5)(Cl)] (**3f**) at 85 °C in two kinds of solvents with different polarities (CCl_4 vs $CDCl_3$ and toluene vs nitrobenzene). Reductive elimination from the complex *cis*-[Au(PPh^{t}Bu$_2$)(Ar_F)(C_6F_5)(Cl)] (**3f**) in the more polar solvent $CDCl_3$ (k_{obs} = 6.80 × 10^{-4} s^{-1}) was roughly 1.7 times faster than that in CCl_4 (k_{obs} = 3.94 × 10^{-4} s^{-1}). Likewise, reductive elimination in nitrobenzene (k_{obs} = 5.27 × 10^{-4} s^{-1}) was 1.4 times faster than that in the less polar solvent toluene (k_{obs} = 3.61 × 10^{-4} s^{-1}).

To further evaluate the effect of solvent polarity, we studied the kinetics of the reductive elimination from *cis*-[Au(PPh^{t}Bu$_2$)(Ar_F)(C_6F_5)(Cl)] (**3f**) in polar solvents DMF and CH_3CN. Interestingly, reductive eliminations from the complex *cis*-[Au(PPh^{t}Bu$_2$)(Ar_F)(C_6F_5)(Cl)] (**3f**) in the more polar solvents DMF (k_{obs} = 5.91 × 10^{-4} s^{-1}) and CH_3CN (k_{obs} = 6.11 × 10^{-4} s^{-1}) were slightly slower than that in $CDCl_3$.

Effect of Added Chloride Anion on C(sp^2)−C(sp^2) Reductive Elimination from *cis*-[Au(PPh^{t}Bu$_2$)(Ar_F)(C_6F_5)(Cl)] (3f). To examine the effect of added chloride anion on the C(sp^2)−C(sp^2) reductive elimination reaction of *cis*-[Au(L)(Ar_F)(Ar′)(Cl)], we studied the reductive elimination of *cis*-[Au(PPh^{t}Bu$_2$)(Ar_F)(C_6F_5)(Cl)] (**3f**) in the presence of different amounts of *n*-Bu_4NCl in $CDCl_3$. The yields of the corresponding biaryl product **4** were not significantly influenced even by the addition of 5.0 equiv of *n*-Bu_4NCl. The rate constant of the reductive elimination of *cis*-[Au(PPh^{t}Bu$_2$)(Ar_F)(C_6F_5)(Cl)] (**3f**) in $CDCl_3$ at 85 °C increased with an increase in the concentration of *n*-Bu_4NCl (0−0.25 M), as shown in Figure 2D. The rate of the reductive elimination from complex **3f** in the presence of 0.25 M of *n*-Bu_4NCl (k_{obs} = 1.01 × 10^{-3} s^{-1}) was roughly 1.6 times faster than that in the absence of *n*-Bu_4NCl (k_{obs} = 6.80 × 10^{-4} s^{-1}). These experiments suggest that the C(sp^2)−C(sp^2) reductive elimination from complex **3f** was not inhibited by the addition of *n*-Bu_4NCl and the increase in the rate constant indicates a kinetic salt effect.

Effect of Added Phosphine Ligand on C(sp^2)−C(sp^2) Reductive Elimination from *cis*-[Au(PPh^{t}Bu$_2$)(Ar_F)(C_6F_5)(Cl)] (3f). To probe the impact of the addition of phosphine ligand on the C(sp^2)−C(sp^2) reductive elimination reaction, we studied the thermolysis of *cis*-[Au(PPh^{t}Bu$_2$)(Ar_F)(C_6F_5)(Cl)] (**3f**) in the presence of various amounts of PPh^{t}Bu$_2$ (0−0.25 M). The yields of the reductive elimination reactions in the presence of 1.0−5.0 equiv of PPh^{t}Bu$_2$ were not affected. Likewise, the rates were not significantly influenced in the presence of different amounts of PPh^{t}Bu$_2$, even though the reductive elimination reactions in the presence of additional ligand were slightly faster, as shown in Figure 2E.

DISCUSSION

Mechanism of C(sp^2)−C(sp^2) Reductive Elimination from *cis*-[Au(L)(Ar_F)(Ar′)(Cl)]. Mechanistically, three possible reaction pathways are proposed for the C(sp^2)−C(sp^2) reductive elimination from diarylgold(III) complexes *cis*-[Au(L)(Ar_F)(Ar′)(Cl)]. In pathway A, a reversible phosphine dissociation generates a three-coordinated Y-shaped Au(III) intermediate, which undergoes C(sp^2)−C(sp^2) reductive elimination by direct means or through an autocatalytic elimination pathway[13h] to give the biaryl product. Alternatively, in pathway B, chloride anion dissociation generates a cationic three-coordinated Y-shaped Au(III) intermediate, followed by a fast reductive elimination to form biaryl product and a cationic Au(I) species, which is trapped by chloride anion to form L−Au−Cl. A third pathway (C) for the C(sp^2)−C(sp^2) reductive elimination from *cis*-[Au(L)(Ar)(Ar′)(Cl)] involves a classic concerted bond-forming process via a three-centered transition state, as shown in Figure 3.

Both the experimental and computational results suggest that, of the three possible mechanistic pathways shown in Figure 3, pathway C is consistent with our experimental data for biaryl reductive elimination from *cis*-[Au(L)(Ar_F)(Ar′)-

DOI: 10.1021/acs.organomet.7b00588
Organometallics XXXX, XXX, XXX−XXX

(Cl)]. Our rationale for proposing such a classic concerted biaryl-forming reductive elimination pathway is described below.

First, pathway A was disfavored because experimental results showed that the $C(sp^2)-C(sp^2)$ reductive elimination from *cis*-[Au(PPh^{t}Bu$_2$)(Ar$_F$)(C$_6$F$_5$)(Cl)] (**3f**) was not inhibited by the addition of free phosphine ligand PPh^{t}Bu$_2$. If a pathway that undergoes an initial reversible dissociation of the phosphine ligand followed by direct or autocatalytic reductive elimination from the resulting three-coordinated Y-shaped diarylgold(III) intermediate is proceeding, an inhibition of the reductive elimination upon the addition of free phosphine ligand should be observed. For example, Kochi's studies showed that the $C(sp^3)-C(sp^3)$ bond-forming reductive elimination from [(Ph$_3$P)ArMe$_3$] was significantly retarded in the presence of 20 mol % of free PPh$_3$.[10] In addition, theoretical calculations showed that dissociation of the phosphine ligand from *cis*-[Au(PPh^{t}Bu$_2$)(Ar$_F$)(C$_6$F$_5$)(Cl)] (**3f**) is a slower process which needs to overcome a much higher energy barrier (43.9 kcal/mol) in comparison to pathway C (22.6 kcal/mol) (Figure 4).

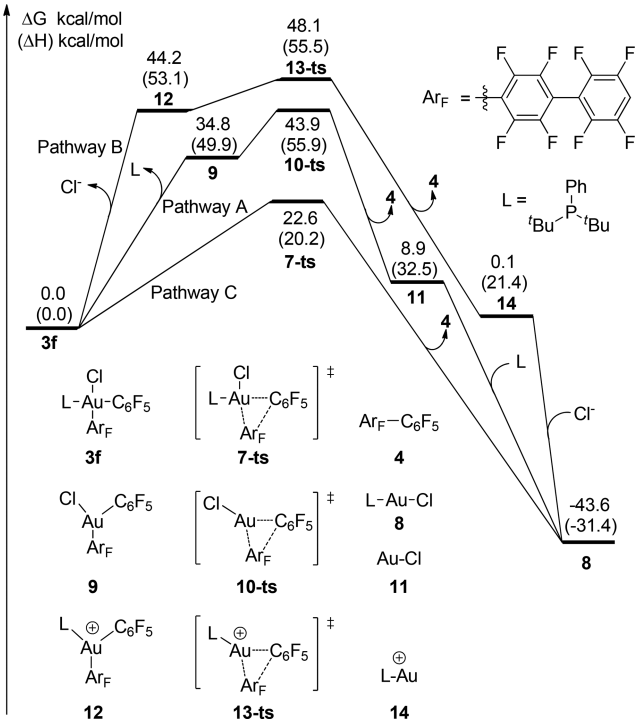

Figure 4. Calculated activation free energies for the $C(sp^2)-C(sp^2)$ reductive elimination of *cis*-[Au(PPh^{t}Bu$_2$)(Ar$_F$)(C$_6$F$_5$)(Cl)] (**3f**).

Second, the observation that the rate of reductive elimination upon the addition of *n*-Bu$_4$NCl was slightly faster than that in the absence of the *n*-Bu$_4$NCl disfavors pathway B. If a reversible dissociation of chloride anion followed by $C(sp^2)-C(sp^2)$ reductive elimination from the resulting cationic three-coordicated Y-shaped Au(III) intermediate takes place, upon addition of *n*-Bu$_4$NCl, a retardation of the rate of the reduction elimination would be expected. The small rate differences in solvents with different polarities also do not support this pathway. Furthermore, DFT calculations showed that the energy barrier for dissociation of chloride anion from *cis*-[Au(PPh^{t}Bu$_2$)(Ar$_F$)(C$_6$F$_5$)(Cl)] (**3f**) is up to 48.1 kcal/mol, which is 25.5 kcal/mol higher than that of pathway C, indicating that the pathway involving the dissociation of chloride anion is disfavored.

Third, if the reductive elimination proceeds via paths A and B, first-order kinetic behaviors would not be observed, which provides additional evidence for the concerted reductive elimination pathway.

Fourth, in pathway C, the calculated actvation free energy and enthalpy of biaryl reductive elimination via transition state **7-ts** are determined to be 22.6 and 20.2 kcal/mol, respectively. The calculated actvation enthalpy is very close to the corresponding experimentally observed activation enthalpy value (21.65 ± 0.77 kcal/mol), which further indicates that the direct biaryl reductive elimination from four-coordinated complex **3f** is favorable in this system.

Effects of the Steric Hindrance of the Phosphine Ligands on $C(sp^2)-C(sp^2)$ Reductive Elimination from *cis*-[Au(L)(Ar$_F$)(Ar′)(Cl)]. Steric hindrance of the phosphine ligands plays an important role in promoting efficient $C(sp^2)-C(sp^2)$ bond-forming reductive elimination from *cis*-[Au(L)(Ar$_F$)(Ar′)(Cl)], as clearly demonstrated by the high-yielding reductive elimination from PCy^{t}Bu$_2$-ligated diarylgold(III) complex **3c** at 85 °C, while the reductive elimination from PCy$_3$- or PCy$_2$^{t}Bu-ligated diarylgold(III) complexes **3a**,**b** required significantly higher reaction temperatures (120−150 °C). PCy$_3$, PCy$_2$^{t}Bu, and PCy^{t}Bu$_2$ have similar electronic properties, yet the steric hindrances of these ligands increase from PCy$_3$ to PCy^{t}Bu$_2$ since the bond angles Cl−Au−C(Ar$_F$) in complexes *cis*-[Au(L)(Ar$_F$)(Ar′)(Cl)] **3a**−**c** decrease from 173.89(14)/174.31(16)° to 171.27(11) and 170.5(8)/169.4(8)°, respectively. As a result, the rates of the $C(sp^2)-C(sp^2)$ reductive elimination from complexes **3a**−**c** increased.

The effect of the steric hindrance of the phosphine ligands was also illustrated by the facile $C(sp^2)-C(sp^2)$ reductive elimination from P^{t}Bu$_3$-ligated diarylgold(III) complex in comparison to that from the analogous di-*tert*-butyl(aryl)-phosphine-ligated diarylgold(III) complex *cis*-[Au(P(*p*-X-C$_6$H$_4$)^{t}Bu$_2$)(Ar$_F$)(Ar′)(Cl)]. The former occurred at room temperature with 81% yield of biaryl **4**, while the latter required a higher temperature (85 °C) to afford the corresponding biaryl and no reductive elimination was observed at room temperature. Sterically, P^{t}Bu$_3$ is bulkier than P(*p*-X-C$_6$H$_4$)^{t}Bu$_2$ (Tolman cone angles: 182° vs 170°), and electronically, P^{t}Bu$_3$ is more strongly donating than P(*p*-X-C$_6$H$_4$)^{t}Bu$_2$. Thus, clearly, the acceleration of reductive elimination from P^{t}Bu$_3$-ligated diarylgold(III) complex is mainly due to the steric effect of the ligand and obviously the steric effect exceeds the decelerating effect resulting from the electron-donating ability of P^{t}Bu$_3$.

To further evaluate the steric effect of the phosphine ligands on the $C(sp^2)-C(sp^2)$ reductive elimination from complexes *cis*-[Au(L)(Ar$_F$)(Ar′)(Cl)], we also studied the steric effect of the ligands on the stability of the transition state by DFT calculation. As shown in Table 6, with a decrease in steric hindrance of the phosphine ligands, the activation free energies of the reductive elimination transition states increased from 24.3 to 31.7 kcal/mol. We reasoned that the steric hindrance of the ligands pushes the Ar$_F$ group away from the phosphine ligand but close to the Ar′ group, thus facilitating the formation of the three-centered transition state. Since the formation of this transition state from the more hindered phosphine-ligated complexes requires a lower energy barrier in comparison to those with less hindered phosphine ligated complexes,

DOI: 10.1021/acs.organomet.7b00588
Organometallics XXXX, XXX, XXX−XXX

Table 6. Calculated Activation Free Energies for the C(sp^2)−C(sp^2) Reductive Elimination from *cis*-[Au(L)(Ar_F)(Ar′)(Cl)]

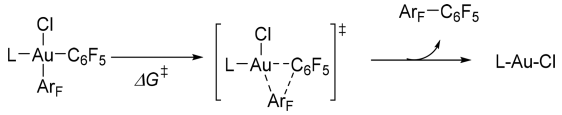

entry	complex	ligand	$\Delta G^{\ddagger}$ (kcal/mol)
1	**3c**	PCy^tBu_2	24.3
2	**3b**	$PCy_2{}^tBu$	26.0
3	**3a**	PCy_3	27.3
4	**3k**	PPh_3	29.3
5	**3l**	PMe_3	31.7

consequently, faster rates for the reductive elimination from the more hindered ligand-ligated complexes were observed.

Electronic Effects of the Phosphine Ligands on the C(sp^2)−C(sp^2) Reductive Elimination from *cis*-[Au(L)(Ar_F)(Ar′)(Cl)]. In contrast to the large differences in rates resulting from changes in the steric hindrance of the ligands, the electronic property of the phosphine ligands has a much smaller effect on the reaction rates. For instance, our studies showed that C(sp^2)−C(sp^2) reductive eliminations occurred more quickly from the more electron-poor di-*tert*-butyl(aryl)-phosphine-ligated diarylgold(III) complexes, although P(*p*-CF_3-C_6H_4)^tBu_2-ligated complex **3h** underwent reductive elimination only 1.5 times faster in comparison to the analogous P(*p*-MeO-C_6H_4)^tBu_2-ligated complex **3d**. These observations are consistent with the conventional electronic effects of the ancillary ligands on the rate of reductive elimination from transition-metal complexes,[1] but the magnitude of the rate difference was small.

An unusual rate difference for reductive elimination reactions from *cis*-[Au($PCy_2{}^tBu$)(Ar_F)(C_6F_5)(Cl)] (**3b**) and *cis*-[Au(P(*p*-MeO-C_6H_4)^tBu_2)(Ar_F)(C_6F_5)(Cl)] (**3d**) was observed. $PCy_2{}^tBu$ is slightly more sterically hindered than P(*p*-MeO-C_6H_4)^tBu_2, which is indicated by the Cl−Au−C(Ar_F) bond angle in the single crystals of complexes **3b,d** (171.27(11) and 172.29(14)°, respectively) that resulted from the steric hindrance of the ligands. Electronically, P(*p*-MeO-C_6H_4)^tBu_2 is more electron withdrawing than $PCy_2{}^tBu$. Yet, the reductive elimination reaction of the complex *cis*-[Au(P(*p*-MeO-C_6H_4)^tBu_2)(Ar_F)(C_6F_5)(Cl)] (**3d**) at 85 °C occurred in over 95% yield after 2 h, while decomposition of *cis*-[Au($PCy_2{}^tBu$)(Ar_F)(C_6F_5)(Cl)] (**3b**) was not detected under the same conditions. A close examination of the single-crystal structure of complex **3d** discloses that the ring centroid distance between the *p*-methoxyphenyl group of the P(*p*-MeO-C_6H_4)^tBu_2 ligand and the 2,2′,3,3′,5,5′,6,6′-octafluoro-1,1′-biphenyl group (Ar_F) of the complex is 3.733(4) Å, which indicates a $\pi-\pi$ interaction between the two aryl groups. Thus, we reasoned that the $\pi-\pi$ interaction between the *p*-methoxyphenyl group of the phosphine ligand and the Ar_F group makes the phosphine ligand much more electron withdrawing. As a result, the reductive elimination from P(*p*-$MeOC_6H_4$)^tBu_2-ligated complex **3d** was accelerated.

CONCLUSION

In summary, we have synthesized a series of well-defined phosphine-ligated diarylgold(III) complexes *cis*-[Au(L)(Ar_F)(Ar′)(Cl)] and systematically studied the C(sp^2)−C(sp^2) reductive elimination process from them. Detailed kinetic studies of the C(sp^2)−C(sp^2) reductive elimination combined with DFT calculations indicate that the biaryl reductive elimination from complexes *cis*-[Au(L)(Ar_F)(Ar′)(Cl)] proceeds through a concerted biaryl-forming pathway from the four-coordinated Au(III) metal center. These studies also disclose that the steric hindrance of the phosphine ligands plays a major role in promoting the reductive elimination from diarylgold(III) complexes, while the electronic properties of the ligands have a much smaller effect. We have also shown that the rates of the C(sp^2)−C(sp^2) reductive elimination were not sensitive to the polarity of the solvents, while more weakly electron withdrawing aryl ligands of the diarylgold(III) complex can accelerate the reaction rate dramatically. In addition, DFT calculations showed that the formation of the three-center transition state is the critical step in the elimination process, which is consistent with the observation that the reaction rates were not sensitive to the polarity of the solvents.

EXPERIMENTAL SECTION

General Information. All glassware was oven- or flame-dried immediately prior to use. Solvents were freshly degassed according to the procedures in *Purification of Laboratory Chemicals* prior to use. Deuterated solvents were purchased from Cambridge Isotope Laboratories, Inc., and were degassed and stored over activated 4 Å molecular sieves. Unless otherwise noted, all other reagents and starting materials were purchased from commercial sources and used without further purification. The ^{1}H, ^{19}F, ^{31}P, and ^{13}C NMR spectra were obtained at 293 K on a 400 or 500 MHz spectrometer, and chemical shifts were recorded relative to the solvent resonance. ^{19}F shifts were determined relative to $CFCl_3$ as an external standard, and low field is positive. Coupling constants are reported in hertz. The following abbreviations were used to explain the multiplicities: s = singlet; d = doublet; t = triplet; q = quartet; m = multiplet; br = broad. Suitable single crystals of complex **2i**, **3a−f,h−j** were selected by optical examination and mounted on a glass fiber. The X-ray diffraction (XRD) data were collected on a Bruker APEX-II CCD diffractometer. The crystal was kept at 130 K during data collection. Using Olex2,[19] the structure was solved with the ShelXT[20] structure solution program using intrinsic phasing and refined with the ShelXL[21] refinement package using least-squares minimization.

General Procedure for the Synthesis of (*p*-X-C_6H_4)^tBu_2P·HBF_4 and ^{t}Bu_2CyP·HBF_4. In a glovebox, di-*tert*-butylchlorophosphine (520 mg, 2.88 mmol), CuI (53 mg, 0.28 mmol), LiBr (48 mg, 0.55 mmol), and dry Et_2O (8.0 mL) were placed in a 100 mL Schlenk tube that was equipped with a stirring bar. (*p*-X-C_6H_4)MgBr or CyMgBr (5.76 mmol, 1.00 mmol/mL in THF solution) was added dropwise at 0 °C in an ice−water bath, and the reaction mixture was stirred at room temperature for 5 h. Then 5.0 mL of HBF_4 (48% aqueous solution) was added dropwise at 0 °C, and the reaction mixture was stirred at room temperature for another 3 h. A 50 mL portion of distilled water and 50 mL of dichloromethane were added, and the organic phase was separated. The aqueous phase was extracted with dichloromethane (2 × 50 mL). The organic phase was combined, dried over anhydrous Na_2SO_4, filtered through Celite, and concentrated in vacuo. The residue was purified by recrystallization in dichloromethane and Et_2O at room temperature.

(p-OMe-C_6H_4)^tBu_2P·HBF_4. According to the general procedure, the compound was obtained as a white solid in 22% yield on a 2.88 mmol scale (230 mg). ^{1}H NMR (400 MHz, $CDCl_3$, 293 K, TMS): δ 7.82 (s, 2 H), 7.16 (d, J = 7.6 Hz, 2 H), 6.86 (d, J = 480.0 Hz, 1 H), 3.91 (s, 3 H), 1.41 (d, J = 17.2 Hz, 18 H). ^{19}F NMR (376 MHz, $CDCl_3$): δ −149.85 (m, 4 F). ^{31}P NMR (162 MHz, $CDCl_3$): δ 43.39 (s, 1 P). ^{13}C NMR (101 MHz, $CDCl_3$): δ 164.7 (d, J = 2.0 Hz), 116.2 (d, J = 13.0 Hz), 105.6, 104.9, 55.8, 34.3 (d, J = 35.0 Hz), 27.6. Anal. Calcd for $C_{15}H_{26}BF_4OP$: C, 52.97; H, 7.70. Found: C, 52.85; H, 7.63.

(p-Me-C_6H_4)^tBu_2P·HBF_4. According to the general procedure, the compound was obtained as a white solid in 81% yield on a 2.88 mmol scale (760 mg). ^{1}H NMR (400 MHz, $CDCl_3$, 293 K, TMS): δ 7.72 (s,

DOI: 10.1021/acs.organomet.7b00588
Organometallics XXXX, XXX, XXX−XXX

2 H), 7.44 (m, 2 H), 6.90 (d, J = 488.0 Hz, 1 H), 2.45 (s, 3 H), 1.49 (d, J = 16.0 Hz, 18 H). ^{19}F NMR (376 MHz, $CDCl_3$): δ −149.80 (m, 4 F). ^{31}P NMR (162 MHz, $CDCl_3$): δ 44.25 (s, 1 P). ^{13}C NMR (101 MHz, $CDCl_3$): δ 146.17 (d, J = 2.7 Hz), 131.11 (d, J = 11.9 Hz), 121.11, 111.37, 34.16 (d, J = 34.6 Hz), 27.55, 21.80. Anal. Calcd for $C_{15}H_{26}BF_4P$: C, 55.58; H, 8.09. Found: C, 55.50; H, 8.07.

(p-Cl-C_6H_4)^{t}Bu$_2$P·HBF$_4$. According to the general procedure, the compound was obtained as a white solid in 31% yield on a 2.88 mmol scale (320 mg). ^{1}H NMR (400 MHz, $CDCl_3$, 293 K, TMS): δ 7.87 (t, J = 8.0 Hz, 2 H), 7.64 (d, J = 8.0 Hz, 2 H), 6.90 (d, J = 488.0 Hz, 1 H), 1.49 (d, J = 16.0 Hz, 18 H). ^{19}F NMR (376 MHz, $CDCl_3$): δ −149.27 (m, 4 F). ^{31}P NMR (162 MHz, $CDCl_3$): δ 44.32 (s, 1 P). ^{13}C NMR (101 MHz, $CDCl_3$) δ 142.0 (d, J = 2.0 Hz), 130.9 (d, J = 12.0 Hz), 114.2, 113.5, 34.3 (d, J = 36.0 Hz), 27.4. Anal. Calcd for $C_{14}H_{23}BClF_4P$: C, 48.80; H, 6.73. Found: C, 48.99; H, 6.62.

^{t}Bu$_2$CyP·HBF$_4$. According to the general procedure, the compound was obtained as a white solid in 52% yield on a 5.76 mmol scale (920 mg). ^{1}H NMR (400 MHz, $CDCl_3$, 293 K, TMS): δ 5.77 (d, J = 466.0 Hz, 1 H), 2.56 (m, 1 H), 2.16 (m, 2 H), 1.89 (m, 2 H), 1.78 (m, 3 H), 1.55 (d, J = 16.0 Hz), 1.41 (m, 3 H). ^{19}F NMR (376 MHz, $CDCl_3$): δ −150.22 (m, 4 F). ^{31}P NMR (162 MHz, $CDCl_3$): δ 46.73 (s, 1 P). ^{13}C NMR (101 MHz, $CDCl_3$): δ 34.6 (d, J = 32.1 Hz), 32.3 (d, J = 34.4 Hz), 29.6 (d, J = 3.8 Hz), 28.3, 27.0 (d, J = 12.1 Hz), 25.2. Anal. Calcd for $C_{14}H_{30}BF_4P$: C, 53.18; H, 9.56. Found: C, 52.88; H, 9.52.

General Procedure for the Preparation of Complexes (L)AuCl. *General Procedure A.*[22] In a glovebox, Cy_3P (672 mg, 2.40 mmol) and Me_2SAuCl (588 mg, 2.00 mmol) were placed in a 25 mL round-bottom flask that was equipped with a stirring bar. A 10 mL portion of dichloromethane was added, and the flask was sealed with a rubber stopper. The mixture was stirred overnight and was then filtered through a short plug of Celite. The solvent was removed under vacuum to give a white solid. Recrystallization of the crude product with dichloromethane and n-pentane gave (Cy_3P)AuCl as a white solid (497 mg, 48%). ^{1}H NMR (400 MHz, $CDCl_3$, 293 K, TMS): δ 1.95 (m, 9 H), 1.82 (m, 6 H), 1.70 (m, 3 H), 1.61 (s, 1 H), 1.42 (m, 6 H), 1.25 (m, 9 H). ^{31}P NMR (162 MHz, $CDCl_3$, 293 K, TMS): δ 54.01 (s, 1 P). ^{13}C NMR (101 MHz, $CDCl_3$, 293 K, TMS): δ 33.3 (d, J = 31.2 Hz), 30.8, 27.0 (d, J = 12.0 Hz), 25.8 ppm.

General Procedure B. In a glovebox, ^{t}Bu$_2$CyP·HBF$_4$ (948 mg, 3.00 mmol) and K_3PO_4 (700 mg, 3.30 mmol) were placed into a 25 mL round-bottom flask that was equipped with a stirring bar. A 5.0 mL portion of THF was placed in the flask, and then the flask was sealed with a rubber stopper. The reaction mixture was stirred at room temperature for 3 h. The mixture was then filtered through a short plug of Celite. Me_2SAuCl (588 mg, 2.00 mmol) and 5.0 mL of dichloromethane were placed in the flask. The reaction mixture was stirred at room temperature overnight. The solvent was removed under vacuum to give a white solid. The residue was purified by recrystallization from dichloromethane and n-pentane to give (Cy^{t}Bu$_2$P)AuCl as a white solid (630 mg, 68%). ^{1}H NMR (400 MHz, $CDCl_3$, 293 K, TMS): δ 2.39 (m, 2 H), 2.03 (m, 1 H), 1.85 (m, 2 H), 1.70 (m, 3 H), 1.44 (d, J = 14.8 Hz, 18 H), 1.26 (m, 3 H). ^{31}P NMR (162 MHz, $CDCl_3$): δ 81.53 (s, 1 P). ^{13}C NMR (101 MHz, $CDCl_3$): δ 38.4 (d, J = 23.6 Hz), 37.3 (d, J = 24.2 Hz), 33.6, 31.0 (d, J = 4.6 Hz), 28.1 (d, J = 11.4 Hz), 26.0 (d, J = 1.3 Hz). Anal. Calcd for $C_{14}H_{29}AuClP$: C, 36.49; H, 6.34. Found: C, 36.39; H, 6.30.

(Cy$_2$^{t}BuP)AuCl. The general procedure A using Cy$_2$^{t}BuP (763 mg, 3.00 mmol) and Me_2SAuCl (588 mg, 2.00 mmol) in 5.0 mL of dichloromethane gave (Cy$_2$^{t}BuP)AuCl as a white solid (672 mg, 69%). ^{1}H NMR (400 MHz, $CDCl_3$, 293 K, TMS): δ 2.03 (m, 6 H), 1.81 (m, 4 H), 1.67 (m, 2 H), 1.54 (m, 4 H), 1.29 (d, J = 14.4 Hz, 9 H), 1.20 (m, 6 H). ^{31}P NMR (162 MHz, $CDCl_3$): δ 67.66 (s, 1 P). ^{13}C NMR (101 MHz, $CDCl_3$): δ 35.0 (d, J = 27.9 Hz), 34.3 (d, J = 28.7 Hz), 32.2, 30.9, 30.2 (d, J = 4.2 Hz), 27.2 (d, J = 7.9 Hz), 27.1 (d, J = 7.9 Hz), 25.7. Anal. Calcd for $C_{16}H_{31}AuClP$: C, 39.48; H, 6.42. Found: C, 39.28; H, 6.23.

(^{t}Bu$_3$P)AuCl.[23] The general procedure A using ^{t}Bu$_3$P (5.3 mL, 10% in n-pentane, 2.3 mmol) and Me_2SAuCl (448 mg, 1.52 mmol) in 10.0 mL of freshly distilled dichloromethane gave (^{t}Bu$_3$P)AuCl as a white solid (539 mg, 82%).^{1}H NMR (400 MHz, $CDCl_3$, 293 K, TMS): δ 1.38 (d, J = 12.0 Hz, 27 H). ^{31}P NMR (162 MHz, $CDCl_3$): δ 90.51 (s, 1 P). ^{13}C NMR (101 MHz, $CDCl_3$): δ 39.4 (d, J = 21.1 Hz), 32.2 (d, J = 4.0 Hz) ppm.

(Ph^{t}Bu$_2$P)AuCl. The general procedure A using Ph^{t}Bu$_2$P (267 mg, 1.20 mmol) and Me_2SAuCl (294 mg, 1.00 mmol) in 5.0 mL of dichloromethane gave (Ph^{t}Bu$_2$P)AuCl as a white solid (340 mg, 62%). ^{1}H NMR (400 MHz, $CDCl_3$, 293 K, TMS): δ 7.93 (t, J = 8.0 Hz, 2 H), 7.50 (m, 1 H), 7.42 (m, 2 H), 1.35 (d, J = 16.0 Hz, 18 H). ^{31}P NMR (162 MHz, $CDCl_3$): δ 79.07 (s, 1 P). ^{13}C NMR (101 MHz, $CDCl_3$): δ 132.0 (d, J = 2.4 Hz), 128.6 (d, J = 10.7 Hz), 127.8, 127.3, 36.4 (d, J = 26.0 Hz), 30.2 (d, J = 6.0 Hz). Anal. Calcd for $C_{14}H_{23}AuClP$: C, 36.98; H, 5.10. Found: C, 37.03; H, 5.12.

((p-MeO-C_6H_4)^{t}Bu$_2$P)AuCl. The general procedure B using (p-MeO-C_6H_4)^{t}Bu$_2$P·HBF$_4$ (156 mg, 0.459 mmol), K_3PO_4 (187 mg, 0.882 mmol), and Me_2SAuCl (118 mg, 0.401 mmol) in 3.0 mL of THF gave ((p-MeO-C_6H_4)^{t}Bu$_2$P)AuCl as a white solid (140 mg, 72%). ^{1}H NMR (400 MHz, $CDCl_3$, 293 K, TMS): δ 7.89 (m, 2 H), 6.96 (d, J = 8.0 Hz, 2 H), 3.84 (s, 3 H), 1.37 (d, J = 16.0 Hz, 18 H). ^{31}P NMR (162 MHz, $CDCl_3$): δ 77.04 (s, 1 P). ^{13}C NMR (101 MHz, $CDCl_3$): δ 162.4 (d, J = 2.0 Hz), 118.4, 117.9, 114.1 (d, J = 12.0 Hz), 55.4, 36.4 (d, J = 27.0 Hz), 30.2 (d, J = 6.0 Hz). Anal. Calcd for $C_{15}H_{25}AuClOP$: C, 37.17; H, 5.20. Found: C, 37.20; H, 5.05.

((p-Me-C_6H_4)^{t}Bu$_2$P)AuCl. The general procedure B using (p-Me-C_6H_4)^{t}Bu$_2$P·HBF$_4$ (211 mg, 0.651 mmol), K_3PO_4 (212 mg, 1.00 mmol), and Me_2SAuCl (147 mg, 0.500 mmol) in 5.0 mL of THF gave ((p-Me-C_6H_4) ^{t}Bu$_2$P)AuCl as a white solid (150 mg, 64%). ^{1}H NMR (400 MHz, $CDCl_3$, 293 K, TMS): δ 7.87 (t, J = 8.0 Hz, 2 H), 7.28 (d, J = 8.0 Hz, 2 H), 2.42 (s, 3 H), 1.41 (d, J = 16.0 Hz, 18 H). ^{31}P NMR (162 MHz, $CDCl_3$): δ 78.06 (s, 1 P). ^{13}C NMR (101 MHz, $CDCl_3$): δ 142.6, 129.4 (d, J = 10.0 Hz), 124.3, 123.8, 36.4 (d, J = 27.0 Hz), 30.2 (d, J = 6.0 Hz), 21.4. Anal. Calcd for $C_{15}H_{25}AuClP$: C, 38.43; H, 5.38. Found: C, 38.31; H, 5.39.

((p-Cl-C_6H_4)^{t}Bu$_2$P)AuCl. The general procedure B using (p-Cl-C_6H_4)^{t}Bu$_2$PH·BF$_4$ (68.8 mg, 0.198 mmol), K_3PO_4 (63.6 mg, 0.300 mmol), and Me_2SAuCl (50.0 mg, 0.170 mmol) in 5.0 mL of THF gave ((p-Cl-C_6H_4)^{t}Bu$_2$P)AuCl as a white solid (52 mg, 62%). ^{1}H NMR (400 MHz, $CDCl_3$, 293 K, TMS): δ 7.95 (t, J = 8.0 Hz, 2 H), 7.49 (d, J = 8.0 Hz, 2 H), 1.42 (d, J = 16.0 Hz, 18 H). ^{31}P NMR (162 MHz, $CDCl_3$): δ 78.26 (s, 1 P). ^{13}C NMR (101 MHz, $CDCl_3$): δ 138.8 (d, J = 2.0 Hz), 128.9 (d, J = 11.0 Hz), 126.4, 125.9, 36.5 (d, J = 26.0 Hz), 30.2 (d, J = 6.0 Hz). Anal. Calcd for $C_{14}H_{22}AuCl_2P$: C, 34.38; H, 4.53. Found: C, 34.47; H, 4.62.

((p-CF_3-C_6H_4)^{t}Bu$_2$P)AuCl. The general procedure A using (p-CF_3-C_6H_4)^{t}Bu$_2$P·HBF$_4$ (348 mg, 1.20 mmol) and Me_2SAuCl (294 mg, 1.00 mmol) in 5.0 mL of dichloromethane gave ((p-CF_3-C_6H_4)^{t}Bu$_2$P)AuCl as a white solid (365 mg, 58%). ^{1}H NMR (400 MHz, $CDCl_3$, 293 K, TMS): δ 8.14 (t, J = 8.0 Hz, 2 H), 7.74 (d, J = 8.0 Hz, 2 H), 1.42 (d, J = 16.0 Hz, 18 H). ^{31}P NMR (162 MHz, $CDCl_3$): δ 79.28 (s, 1 P). ^{19}F NMR (376 MHz, $CDCl_3$): δ −63.23 (s, 3 F). ^{13}C NMR (101 MHz, $CDCl_3$): δ 133.8 (q, J = 33.0 Hz), 132.6, 132.1, 125.3 (m), 124.7 (q, J = 271.0 Hz), 36.6 (d, J = 26.0 Hz), 30.2 (d, J = 6.0 Hz). Anal. Calcd for $C_{15}H_{22}AuClF_3P$: C, 34.47; H, 4.24. Found: C, 34.48; H, 4.11.

General Procedure for the Preparation of Complexes (L)Au(octafluorobiphenyl) (1a−h).[15] (Cy_3P)AuCl (256 mg, 0.500 mmol), Ag_2O (290 mg, 1.25 mmol), K_2CO_3 (121 mg, 1.75 mmol), PivOH (128 mg, 1.25 mmol), and octafluorobiphenyl (596 mg, 1.00 mmol) were placed in an oven-dried 25.0 mL Schlenk tube that was equipped with a stirring bar under Ar. Then 4.0 mL of freshly distilled DMF was added and the reaction mixture was stirred at 55 °C overnight. The mixture was then filtered through a short plug of Celite. The solvent was removed under vacuum. The residue was purified by flash chromatography on silica gel (n-pentane/dichloromethane 10/1) and further purified by recrystallization by dichloromethane and n-pentane to give (Cy_3P)Au(octafluorobiphenyl) (**1a**) as a white solid (210 mg, 54%). ^{1}H NMR (400 MHz, CD_2Cl_2, 293 K, TMS): δ 7.21 (m, 1 H), 2.18−2.03 (m, 9 H), 1.86 (d, J = 12.0 Hz, 6 H), 1.73 (d, J = 8.0 Hz, 3 H), 1.54 (q, J = 12.0 Hz, 3 H), 1.39−1.21 (m, 9 H). ^{19}F NMR (376 MHz, CD_2Cl_2): δ −118.16 (m, 2 F), −140.25 (m, 4 F), −141.60 (m, 2 F). ^{31}P NMR (162 MHz, CD_2Cl_2):

DOI: 10.1021/acs.organomet.7b00588
Organometallics XXXX, XXX, XXX−XXX

δ 56.54−56.36 (m, 1 P). Anal. Calcd for $C_{30}H_{34}AuF_8P$: C, 46.52; H, 4.42. Found: C, 46.54; H, 4.35.

*(Cy_2^tBuP)Au(octafluorobiphenyl) (**1b**).* The general procedure using (Cy_2^tBuP)AuCl (488 mg, 1.44 mmol), Ag_2O (249 mg, 1.07 mmol), K_2CO_3 (345 mg, 2.50 mmol), PivOH (364 mg, 3.60 mmol), and octafluorobiphenyl (852 mg, 2.86 mmol) in 3.0 mL of freshly distilled DMF gave (Cy_2^tBuP)Au(octafluorobiphenyl) (**1b**) as a white solid (460 mg, 43%). ^{1}H NMR (400 MHz, $CDCl_3$, 293 K, TMS): δ 7.18 (m, 1 H), 2.26 (m, 4 H), 2.14 (m, 2 H), 1.92 (m, 4 H), 1.70 (m, 6 H), 1.43 (d, *J* = 14.0 Hz, 9 H), 1.33 (m, 6 H). ^{19}F NMR (376 MHz, $CDCl_3$): δ −117.08 (m, 2 F), −138.62 (m, 2 F), −139.04 (m, 2 F), −140.37 (m, 2 F). ^{31}P NMR (162 MHz, $CDCl_3$): δ 69.46 (m, 1 P). Anal. Calcd for $C_{28}H_{32}AuF_8P$: C, 44.93; H, 4.31. Found: C, 45.03; H, 4.31.

*(Cy^tBu_2P)Au(octafluorobiphenyl) (**1c**).* The general procedure using (Cy^tBu_2P)AuCl (660 mg, 1.43 mmol), Ag_2O (249 mg, 1.07 mmol), K_2CO_3 (345 mg, 2.50 mmol), PivOH (364 mg, 3.60 mmol), and octafluorobiphenyl (852 mg, 2.86 mmol) in 3.0 mL of freshly distilled DMF gave (Cy^tBu_2P)Au(octafluorobiphenyl) (**1c**) as a white solid (680 mg, 66%). ^{1}H NMR (400 MHz, $CDCl_3$, 293 K, TMS): δ 7.18 (m, 1 H), 2.48 (s, 2 H), 2.12 (m, 1 H), 1.91 (m, 2 H), 1.77 (m, 3 H), 1.52 (d, *J* = 16.8 Hz, 18 H), 1.33 (m, 3 H). ^{19}F NMR (376 MHz, $CDCl_3$): δ −117.00 (m, 2 F), −138.64 (m, 2 F), −139.03 (m, 2 F), −140.39 (m, 2 F). ^{31}P NMR (162 MHz, $CDCl_3$): δ 82.36 (m, 1 P). Anal. Calcd for $C_{26}H_{30}AuF_8P$: C, 43.23; H, 4.19. Found: C, 43.33; H, 4.19.

*((p-MeO-C_6H_4)$^tBu_2$P)Au(octafluorobiphenyl) (**1d**).* The general procedure using ((*p*-OMe-C_6H_4)$^tBu_2$P)AuCl (131 mg, 0.270 mmol), Ag_2O (63 mg, 0.27 mmol), K_2CO_3 (65 mg, 0.47 mmol), PivOH (69 mg, 0.68 mmol), and octafluorobiphenyl (161 mg, 0.540 mmol) in 3.0 mL of freshly distilled DMF gave ((*p*-MeO-C_6H_4)$^tBu_2$P)Au(octafluorobiphenyl) (**1d**) as a white solid (85 mg, 42%). ^{1}H NMR (400 MHz, $CDCl_3$, 293 K, TMS): δ 7.96 (s, 2 H), 7.15 (m, 2 H), 7.00 (d, *J* = 8.0 Hz, 2 H), 3.85 (s, 3 H), 1.43 (d, *J* = 16.0, 18 H). ^{19}F NMR (376 MHz, $CDCl_3$): δ −116.96 (m, 2 F), −138.65 (m, 2 F), −139.01 (m, 2 F), −140.31 (m, 2 F). ^{31}P NMR (162 MHz, $CDCl_3$): δ 78.85 (m, 1 P). Anal. Calcd for $C_{27}H_{26}AuF_8OP$: C, 43.45; H, 3.51. Found: C, 43.56; H, 3.56.

*((p-Me-C_6H_4)$^tBu_2$P)Au(octafluorobiphenyl) (**1e**).* The general procedure using ((*p*-Me-C_6H_4)$^tBu_2$P)AuCl (400 mg, 0.853 mmol), Ag_2O (199 mg, 0.858 mmol), K_2CO_3 (208 mg, 1.45 mmol), PivOH (219 mg, 2.15 mmol), and octafluorobiphenyl (513 mg, 1.72 mmol) in 4.0 mL of freshly distilled DMF gave ((*p*-Me-C_6H_4)$^tBu_2$P)Au(octafluorobiphenyl) (**1e**) as a white solid (560 mg, 90%). ^{1}H NMR (400 MHz, $CDCl_3$, 293 K, TMS): δ 7.96 (s, 2 H), 7.33 (d, *J* = 8.0 Hz, 2 H), 7.19 (m, 1 H), 2.45 (s, 3 H), 1.48 (d, *J* = 16.0 Hz, 18 H). ^{19}F NMR (376 MHz, $CDCl_3$): δ −116.94 (m, 2 F), −138.59 (m, 2 F), −138.97 (m, 2 F), −140.27 (m, 2 F). ^{31}P NMR (162 MHz, $CDCl_3$): δ 78.74 (m, 1 P). Anal. Calcd for $C_{27}H_{26}AuF_8P$: C, 44.40; H, 3.59. Found: C, 44.63; H, 3.58.

*(Ph^tBu_2P)Au(octafluorobiphenyl) (**1f**).* The general procedure using (Ph^tBu_2P)AuCl (454 mg, 1.00 mmol), Ag_2O (174 mg, 0.750 mmol), K_2CO_3 (241 mg, 1.75 mmol), PivOH (255 mg, 2.50 mmol), and octafluorobiphenyl (596 mg, 2.00 mmol) in 3.0 mL of freshly distilled DMF gave (Ph^tBu_2P)Au(octafluorobiphenyl) (**1f**) as a white solid (366 mg, 51%). ^{1}H NMR (400 MHz, $CDCl_3$, 293 K, TMS): δ 8.04 (s, 2 H), 7.49 (m, 3 H), 7.15 (m, 1 H), 1.45 (d, J = 16.0 Hz, 18 H). ^{19}F NMR (376 MHz, $CDCl_3$): δ −117.00 (m, 2 F), −138.64 (m, 2 F), −139.02 (m, 2 F), −140.30 (m, 2 F). ^{31}P NMR (162 MHz, $CDCl_3$): δ 79.79 (m, 1 P). Anal. Calcd for $C_{26}H_{24}AuF_8P$: C, 43.59; H, 3.38. Found: C, 43.55; H, 3.40.

*((p-Cl-C_6H_4)$^tBu_2$P)Au(octafluorobiphenyl) (**1g**).* The general procedure using ((*p*-Cl-C_6H_4)$^tBu_2$P)AuCl (270 mg, 0.552 mmol), Ag_2O (96 mg, 0.41 mmol), K_2CO_3 (133 mg, 0.964 mmol), PivOH (140 mg, 1.372 mmol), and octafluorobiphenyl (328 mg, 1.10 mmol) in 3.0 mL of freshly distilled DMF gave ((*p*-Cl-C_6H_4)$^tBu_2$P)Au(octafluorobiphenyl) (**1g**) as a white solid (270 mg, 65%). ^{1}H NMR (400 MHz, $CDCl_3$, 293 K, TMS): δ 7.99 (s, 2 H), 7.48 (d, *J* = 8.0 Hz, 2 H), 7.16 (m, 1 H), 1.44 (d, *J* = 16.0 Hz, 18 H). ^{19}F NMR (376 MHz, $CDCl_3$): δ −116.93 (m, 2 F), −138.67 (m, 2 F), −138.87 (m, 2 F), −140.12 (m, 2 F). ^{31}P NMR (162 MHz, $CDCl_3$): δ 79.30 (m, 1 P). Anal. Calcd for $C_{26}H_{23}AuClF_8P$: C, 41.59; H, 3.09. Found: C, 41.61; H, 3.09.

*((p-CF_3-C_6H_4)$^tBu_2$P)Au(octafluorobiphenyl) (**1h**).* The general procedure using (*p*-CF_3-C_6H_4)$^tBu_2$P)AuCl (783 mg, 1.50 mmol), Ag_2O (309 mg, 1.13 mmol), K_2CO_3 (362 mg, 2.63 mmol), PivOH (382 mg, 3.75 mmol), and octafluorobiphenyl (894 mg, 3.00 mmol) in 5.0 mL of freshly distilled DMF gave ((*p*-CF_3-C_6H_4)$^tBu_2$P)Au(octafluorobiphenyl) (**1h**) as a white solid (788 mg, 67%). ^{1}H NMR (400 MHz, $CDCl_3$, 293 K, TMS): δ 8.02 (s, 2 H), 7.51 (d, *J* = 8.0 Hz, 2 H), 7.19 (m, 1 H), 1.47 (d, *J* = 16.0 Hz, 18 H). ^{19}F NMR (376 MHz, $CDCl_3$): δ −68.46 (s, 3 F), −122.25 (m, 2 F), −143.89 (m, 2 F), −144.15 (m, 2 F), −145.33 (m, 2 F). ^{31}P NMR (162 MHz, $CDCl_3$): δ 80.36 (m, 1 P). Anal. Calcd for $C_{27}H_{23}AuF_{11}P$: C, 41.34; H, 2.96. Found: C, 41.15; H, 3.04.

*(Ph_3P)Au(octafluorobiphenyl) (**1i**).* The general procedure using Ph_3PAuCl (306 mg, 0.619 mmol), Ag_2O (100 mg, 0.433 mmol), K_2CO_3 (138 mg, 1.00 mmol), PivOH (146 mg, 1.43 mmol), and octafluorobiphenyl (895 mg, 2.48 mmol) in 3.0 mL of freshly distilled DMF gave (Ph_3P)Au(octafluorobiphenyl) (**1i**) as a white solid (446 mg, 67%). ^{1}H NMR (400 MHz, CD_2Cl_2, 293 K, TMS): δ 7.68−7.43 (m, 15 H), 7.30−7.13 (m, 1 H). ^{19}F NMR (376 MHz, CD_2Cl_2): δ −115.11 (m, 2 F), −137.62 (m, 4 F), −138.75 (m, 2 F). ^{31}P NMR (162 MHz, CD_2Cl_2): δ 43.82 (m, 1 P). Anal. Calcd for $C_{30}H_{16}AuF_8P$: C, 47.67; H, 2.13. Found: C, 47.71; H, 2.12.

($^tBu_3P$)Au(octafluorobiphenyl). The general procedure using ($^tBu_3P$)AuCl (217 mg, 0.500 mmol), Ag_2O (290 mg, 1.25 mmol), K_2CO_3 (121 mg, 0.880 mmol), PivOH (128 mg, 1.25 mmol), and octafluorobiphenyl (298 mg, 1.00 mmol) in 4.0 mL of freshly distilled DMF gave ($^tBu_3P$)Au(octafluorobiphenyl) as a white solid (102 mg, 28%). ^{1}H NMR (400 MHz, CD_2Cl_2, 293 K, TMS): δ 7.17−7.09 (m, 1 H), 1.46 (d, *J* = 12.0 Hz, 27 H) ppm; ^{19}F NMR (376 MHz, CD_2Cl_2): δ −115.52 (m, 2 F), −137.64 (m, 4 F), −139.04 (m, 2 F). ^{31}P NMR (162 MHz, CD_2Cl_2): δ 93.84 (m, 1 P). Anal. Calcd for $C_{24}H_{28}AuF_8P$: C, 41.39; H, 4.05. Found: C, 41.40; H, 3.90.

General Procedure for the Preparation of Complexes *cis*-(L)Au(octafluorobiphenyl)Cl_2 (2a−h).[13d,16] The complex (Cy_3P)-Au(octafluorobiphenyl) (**1a**; 600 mg, 0.775 mmol) and $PhICl_2$ (742 mg, 2.70 mmol) were placed in an oven-dried Schlenk tube that was equipped with a stirring bar. A 5.0 mL portion of $CHCl_3$ was added, and the reaction mixture was stirred at 45 °C for 3 h. The solvent was removed under vacuum, and the residue was purified by flash chromatography on silica gel (*n*-pentane/dichloromethane 10/1 to 1/1) and further purified by recrystallization of dichloromethane and *n*-pentane to give *cis*-(Cy_3P)Au(octafluorobiphenyl)Cl_2 (**2a**) as a white solid (154 mg, 23%). ^{1}H NMR (400 MHz, CD_2Cl_2, 293 K, TMS): δ 7.18 (m, 1 H), 2.76 (q, *J* = 4.1 Hz, 3 H), 1.94 (s, 6 H), 1.81 (s, 6 H), 1.72−1.60 (m, 9 H), 1.27 (s, 9 H). ^{19}F NMR (376 MHz, CD_2Cl_2): δ −127.25 (m, 2 F), −139.65 to −139.92 (m, 4 F), −140.05 (m, 2 F). ^{31}P NMR (162 MHz, CD_2Cl_2): δ 66.21 (s, 1 P). Anal. Calcd for $C_{30}H_{34}AuCl_2F_8P$: C, 42.62; H, 4.05. Found: C, 42.16; H, 4.03.

*cis-(Cy_2^tBuP)Au(octafluorobiphenyl)Cl_2 (**2b**).* The general procedure using the complex (Cy_2^tBuP)Au(octafluorobiphenyl) (**1b**; 202 mg, 0.270 mmol) and $PhICl_2$ (110 mg, 0.400 mmol) in 3.0 mL of $CHCl_3$ gave *cis*-(Cy_2^tBuP)Au(octafluorobiphenyl)Cl_2 (**2b**) as a white solid (176 mg, 80%). ^{1}H NMR (400 MHz, $CDCl_3$, 293 K, TMS): δ 7.22 (m, 1 H), 2.96 (s, 2 H), 2.33 (s, 2 H), 2.00 (s, 2 H), 1.80 (s, 4 H), 1.71 (m, 2 H), 1.62 (d, *J* = 16.0 Hz, 9 H), 1.50 (m, 2 H), 1.50−1.16 (br, 8 H). ^{19}F NMR (376 MHz, $CDCl_3$): δ −119.92 (m, 2 F), −137.11 (m, 1 F), −137.39 (m, 3 F), −138.26 (m, 1 F), −139.52 (m, 1 F). ^{31}P NMR (162 MHz, $CDCl_3$): δ 74.98 (s, 1 P). Anal. Calcd for $C_{28}H_{32}AuCl_2F_8P$: C, 41.04; H, 3.94. Found: C, 41.29; H, 4.06.

*cis-(Cy^tBu_2P)Au(octafluorobiphenyl)Cl_2 (**2c**).* The general procedure using the complex (Cy^tBu_2P)Au(octafluorobiphenyl) (**1c**; 115 mg, 0.160 mmol) and $PhICl_2$ (66 mg, 0.24 mmol) in 3.0 mL of $CHCl_3$ gave *cis*-(Cy^tBu_2P)Au(octafluorobiphenyl)Cl_2 (**2c**) as a white solid (78 mg, 63%). ^{1}H NMR (400 MHz, $CDCl_3$, 293 K, TMS): δ 7.22 (m, 2 H), 2.23 (s, 2 H), 1.82−1.61 (br, 23 H), 1.20 (m, 2 H), 0.73 (br, 2 H). ^{19}F NMR (376 MHz, $CDCl_3$): δ −118.30 (m, 1 F), −137.18 (m, 1 F), −137.47 (m, 1 F), −137.61 (m, 2 F), −138.35 (m, 1 F), −139.55 (m,

DOI: 10.1021/acs.organomet.7b00588
Organometallics XXXX, XXX, XXX−XXX

1 F). ^{31}P NMR (162 MHz, $CDCl_3$): δ 89.25 (br, 1 P). Anal. Calcd for $C_{26}H_{30}AuCl_2F_8P$: C, 39.36; H, 3.81. Found: C, 39.33; H, 3.81.

*cis-((p-MeO-C$_6$H$_4$)^{t}Bu$_2$P)Au(octafluorobiphenyl)Cl$_2$ (**2d**).* The general procedure using the complex ((*p*-OMe-C_6H_4)^{t}Bu$_2$P)Au(octafluorobiphenyl) (**1d**; 66 mg, 0.089 mmol) and $PhICl_2$ (49 mg, 0.18 mmol) in 3.0 mL of $CHCl_3$ gave *cis*-((*p*-MeO-C_6H_4)^{t}Bu$_2$P)Au(octafluorobiphenyl)Cl_2 (**2d**) as a white solid (45 mg, 62%). ^{1}H NMR (400 MHz, $CDCl_3$, 293 K, TMS): δ 7.66 (t, J = 8.0 Hz, 2 H), 7.18 (m, 1 H), 6.83 (dd, J = 8.0, 4.0 Hz, 2 H), 3.78 (s, 3 H), 1.71 (d, J = 16.0 Hz, 18 H). ^{19}F NMR (376 MHz, $CDCl_3$): δ −119.79 (m, 2 F), −137.16 (m, 1 F), −137.59 (m, 1 F), −137.77 (m, 2 F), −138.82 (m, 1 F), −139.72 (m, 1 F). ^{31}P NMR (162 MHz, $CDCl_3$): δ 74.44 (s, 1 P). Anal. Calcd for: $C_{27}H_{26}AuCl_2F_8OP$, 39.37; H, 3.28. Found: C, 39.68; H, 3.21.

*cis-((p-Me-C$_6$H$_4$)^{t}Bu$_2$P)Au(octafluorobiphenyl)Cl$_2$ (**2e**).* The general procedure using the complex ((*p*-Me-C_6H_4)^{t}Bu$_2$P)Au(octafluorobiphenyl) (**1e**; 197 mg, 0.270 mmol) and $PhICl_2$ (148 mg, 0.538 mmol) in 3.0 mL of $CHCl_3$ gave *cis*-((*p*-Me-C_6H_4)^{t}Bu$_2$P)Au(octafluorobiphenyl)Cl_2 (**2e**) as a white solid (210 mg, 97%). ^{1}H NMR (400 MHz, $CDCl_3$, 293 K, TMS): δ 7.61 (t, J = 9.0 Hz, 2 H), 7.18 (m, 1 H), 7.13 (d, J = 8.0 Hz, 2 H), 2.29 (s, 3 H), 1.71 (d, J = 16.8 Hz, 18 H). ^{19}F NMR (376 MHz, $CDCl_3$): δ −119.77 (m, 2 F), −137.04 (m, 1 F), −137.49 (m, 1 F), −137.91 (m, 2 F), −138.68 (m, 1 F), −139.69 (m, 1 F). ^{31}P NMR (162 MHz, $CDCl_3$): δ 74.75 (s, 1 P). Anal. Calcd for $C_{30}H_{32}AuCl_2F_8P$: C, 40.47; H, 3.27. Found: C, 40.13; H, 3.11.

*cis-(Ph^{t}Bu$_2$P)Au(octafluorobiphenyl)Cl$_2$ (**2f**).* The general procedure using the complex (Ph^{t}Bu$_2$P)Au(octafluorobiphenyl) (**1f**; 143 mg, 0.200 mmol) and $PhICl_2$ (110 mg, 0.400 mmol) in 3.0 mL of $CHCl_3$ gave *cis*-(Ph^{t}Bu$_2$P)Au(octafluorobiphenyl)Cl_2 (**2f**) as a white solid (110 mg, 70%). ^{1}H NMR (400 MHz, $CDCl_3$, 293 K, TMS): δ 7.74 (t, J = 8.0 Hz, 2 H), 7.42 (m, 1 H), 7.33 (m 2 H), 7.18 (m, 1 H), 1.73 (d, J = 16.0 Hz, 18 H). ^{19}F NMR (376 MHz, $CDCl_3$): δ −119.93 (m, 2 F), −137.16 (m, 1 F), −137.60 (m, 1 F), −137.83 (m, 2 F), −138.56 (m, 1 F), −139.08 (m, 1 F). ^{31}P NMR (162 MHz, $CDCl_3$): δ 74.22 (m, 1 P). Anal. Calcd for $C_{26}H_{24}AuCl_2F_8P$: C, 39.67; H, 3.07. Found: C, 39.68; H, 3.11.

*cis-((p-Cl-C$_6$H$_4$)^{t}Bu$_2$P)Au(octafluorobiphenyl)Cl$_2$ (**2g**).* The general procedure using the complex ((*p*-Cl-C_6H_4)^{t}Bu$_2$P)Au(octafluorobiphenyl) (**1g**; 203 mg, 0.270 mmol) and $PhICl_2$ (148 mg, 0.540 mmol) in 3.0 mL of $CHCl_3$ gave *cis*-((*p*-Cl-C_6H_4)^{t}Bu$_2$P)Au(octafluorobiphenyl)Cl_2 (**2g**) as a white solid (170 mg, 71%). ^{1}H NMR (400 MHz, $CDCl_3$, 293 K, TMS): δ 7.69 (t, J = 8.0 Hz, 2 H), 7.12 (dd, J = 8.0, 2.0 Hz, 2 H), 7.20 (m, 1 H), 1.78 (d, J = 16.0 Hz, 18 H). ^{19}F NMR (376 MHz, $CDCl_3$): δ −119.57 (m, 2 F), −137.74 (m, 3 F), −137.61 (m, 1 F), −138.40 (m, 1 F), −139.05 (m, 1 F). ^{31}P NMR (162 MHz, $CDCl_3$): δ 76.05 (s, 1 P). Anal. Calcd for $C_{26}H_{23}AuCl_3F_8P$: C, 38.00; H, 2.82. Found: C, 37.89; H, 2.95.

*cis-((p-CF$_3$-C$_6$H$_4$)^{t}Bu$_2$P)Au(octafluorobiphenyl)Cl$_2$ (**2h**).* The general procedure using the complex ((*p*-CF_3-C_6H_4)^{t}Bu$_2$P)Au(octafluorobiphenyl) (**1h**; 235 mg, 0.300 mmol) and $PhICl_2$ (165 mg, 0.600 mmol) in 3.0 mL of $CHCl_3$ gave *cis*-((*p*-CF_3-C_6H_4)^{t}Bu$_2$P)Au(octafluorobiphenyl)Cl_2 (**2h**) as a white solid (130 mg, 51%). ^{1}H NMR (400 MHz, $CDCl_3$, 293 K, TMS): δ 7.97 (t, J = 8.0 Hz, 2 H), 7.69 (d, J = 8.0, 2 H), 7.24 (m, 1 H), 1.73 (d, J = 16.0 Hz, 18 H). ^{19}F NMR (376 MHz, $CDCl_3$): δ −63.76 (d, J = 5.3 Hz, 3 F), −119.39 (m, 2 F), −137.07 (m, 2 F), −137.28 (m, 1 F), −137.54 (m, 1 F), −138.46 (m, 1 F), −139.24 (m, 1 F). ^{31}P NMR (162 MHz, $CDCl_3$): δ 76.40 (s, 1 P). Anal. Calcd for $C_{27}H_{23}AuCl_2F_{11}P$: C, 37.92; H, 2.71. Found: C, 37.74; H, 2.79.

cis-(^{t}Bu$_3$P)Au(octafluorobiphenyl)Cl$_2$. The general procedure using complex (^{t}Bu$_3$P)Au(octafluorobiphenyl) (63.1 mg, 0.0734 mmol) and $PhICl_2$ (99.8 mg, 0.363 mmol) in 3.0 mL of $CHCl_3$ gave *cis*-(^{t}Bu$_3$P)Au(octafluorobiphenyl)Cl_2 as a yellow solid (39 mg, 54%). ^{1}H NMR (400 MHz, CD_2Cl_2, 293 K, TMS): δ 7.22 (m, 1 H), 1.61 (d, J = 16.0 Hz, 27 H) ppm; ^{19}F NMR (376 MHz, CD_2Cl_2): δ −119.75 (m, 2 F), −138.17 to −138.69 (m, 4 F), −139.14 (m, 1 F), −139.84 (m, 1 F). ^{31}P NMR (162 MHz, CD_2Cl_2): δ 107.54 (s, 1 P). Anal. Calcd for $C_{24}H_{28}AuCl_2F_8PS$: C, 37.57; H, 3.68. Found: C, 37.54; H, 3.67.

*cis-(Ph$_3$P)Au(octafluorobiphenyl)Cl$_2$·CH$_2$Cl$_2$ (**2i**).* The general procedure using the complex Ph_3PAu(octafluorobiphenyl) (244 mg, 0.323 mmol) and $PhICl_2$ (310 mg, 1.13 mmol) in 10.0 mL of $CHCl_3$ gave *cis*-(Ph_3P)Au(octafluorobiphenyl)Cl_2·CH_2Cl_2 (**2i**) as a white solid (220 mg, 82%). ^{1}H NMR (400 MHz, CD_2Cl_2, 293 K, TMS): δ 7.74−7.39 (m, 15 H), 7.28−7.17 (m, 1 H), 5.38 (s, 2 H). ^{19}F NMR (376 MHz, CD_2Cl_2): δ −122.18 (m, 2 F), −135.73 (m, 4 F), −136.59 (m, 3 F), −137.15 (m, 1F). ^{31}P NMR (162 MHz, CD_2Cl_2): δ 36.32 (m, 1 P). Anal. Calcd for $C_{31}H_{18}AuCl_4F_8P$: C, 40.82; H, 1.99. Found: C, 40.78; H, 2.08.

General Procedure for the Preparation of Complexes *cis*-[Au(L)(octafluorobiphenyl)(Ar′)(Cl)] (3a−h). In a glovebox, AgF (56 mg, 0.44 mmol), $TMSC_6F_5$ (126 μL, 0.660 mmol), and MeCN (2.0 mL) were placed in a 4.0 mL Schlenk tube that was equipped with a stirring bar. The reaction mixture was stirred in the dark for 3 h. Complex **2a** (200 mg, 0.254 mmol) was placed in the Schlenk tube, and the reaction mixture was stirred at room temperature in the dark for 2 h. The mixture was then filtered through a short plug of Celite. The solvent was removed under vacuum. The residue was purified by flash chromatography on silica gel (*n*-pentane/dichloromethane 50/1 to 10/1) to give *cis*-[Au(PCy_3) (octafluorobiphenyl)(C_6F_5)(Cl)] (**3a**) as a white solid (130 mg, 56%). ^{1}H NMR (400 MHz, $CDCl_3$, 293 K, TMS): δ 7.21 (m, 1 H), 2.44 (q, J = 11.6 Hz, 6 H), 1.96 (s, 6 H), 1.87 (d, J = 11.6 Hz, 6 H), 1.74−1.63 (br, 9 H), 1.27−1.10 (br, 9 H). ^{19}F NMR (376 MHz, $CDCl_3$): δ −118.67 (m, 2 F), −123.58 (m, 2 F), −137.30 (m, 2 F), −137.58 (m, 2 F), −138.10 (m, 1 F), −139.32 (m, 1 F), −157.00 (m, 1 F), −160.95 (m, 2 F). ^{31}P NMR (162 MHz, $CDCl_3$): δ 37.60 (s, 1 P). Anal. Calcd for $C_{36}H_{34}AuClF_{13}P$: C, 44.26; H, 3.51. Found: C, 44.68; H, 3.75.

*cis-[Au(PCy$_2$^{t}Bu)(octafluorobiphenyl)(C$_6$F$_5$)(Cl)] (**3b**).* The general procedure using AgF (56 mg, 0.44 mmol), $TMSC_6F_5$ (126 μL, 0.660 mmol), and *cis*-(Cy_2^{t}BuP)Au(octafluorobiphenyl)Cl_2 (**2b**; 200 mg, 0.244 mmol) in MeCN (2.0 mL) gave *cis*-[Au(PCy_2^{t}Bu)(octafluorobiphenyl)(C_6F_5)(Cl)] (**3b**) as a white solid (125 mg, 54%). ^{1}H NMR (400 MHz, $CDCl_3$, 293 K, TMS): δ 7.21 (m, 1 H), 2.81 (q, J = 11.5 Hz, 2 H), 2.28 (s, 2 H), 1.96 (d, J = 14.0 Hz, 2 H), 1.78 (s, 4 H), 1.71 (d, J = 14.4 Hz, 2 H), 1.57 (d, J = 14.8 Hz, 9 H), 1.52−1.50 (br, 2 H), 1.48−1.24 (br, 8 H). ^{19}F NMR (376 MHz, $CDCl_3$): δ −118.63 (m, 2 F), −123.96 (m, 2 F), −137.34 to −137.68 (m, 4 F), −138.11(m, 1 F), −139.23 (m, 1 F), −157.03 (t, J = 19.9 Hz, 1 F), −160.77 (m, 2 F). ^{31}P NMR (202 MHz, $CDCl_3$): δ 49.51 (s, 1 P). Anal. Calcd for $C_{34}H_{32}AuClF_{13}P$: C, 42.94; H, 3.39. Found: C, 43.28; H, 2.96.

*cis-[Au(PCy^{t}Bu$_2$)(octafluorobiphenyl)(C$_6$F$_5$)(Cl)] (**3c**).* The general procedure using AgF (56 mg, 0.44 mmol), $TMSC_6F_5$ (126 μL, 0.660 mmol), and *cis*-($Cy^{t}Bu_2P$)Au(octafluorobiphenyl)Cl_2 (**2c**; 100 mg, 0.126 mmol) in MeCN (2.0 mL) gave *cis*-[Au($PCy^{t}Bu_2$)(octafluorobiphenyl)(C_6F_5)(Cl)] (**3c**) as a white solid (72 mg, 62%). ^{1}H NMR (400 MHz, $CDCl_3$, 293 K, TMS): δ 7.20 (m, 1 H), 2.20 (s, 2 H), 1.79 (d, J = 13.2 Hz, 2 H), 1.74−1.54 (m, 23 H), 1.21 (q, J = 15.1 Hz, 2 H), 0.89 (s, 2H); ^{19}F NMR (376 MHz, $CDCl_3$): δ −116.98 (m, 1.3 F), −123.95 (m, 2 F), −137.33 (m, 2 F), −137.57 (m, 2 F), −138.21 (m, 1 F), −139.38 (m, 1 F), −157.00 (t, J = 20.1 Hz, 1 F), −160.71 (m, 2 F). ^{31}P NMR (202 MHz, $CDCl_3$): δ 65.42 (s, 1 P). Anal. Calcd for $C_{32}H_{30}AuClF_{13}P$: C, 41.55; H, 3.27. Found: C, 41.30; H, 3.44.

*cis-[Au(P(p-OMe-C$_6$H$_4$)^{t}Bu$_2$)(octafluorobiphenyl)(C$_6$F$_5$)(Cl)] (**3d**).* The general procedure using AgF (56 mg, 0.44 mmol), $TMSC_6F_5$ (126 μL, 0.660 mmol), and *cis*-((*p*-$MeOC_6H_4$)^tBu_2P)Au(octafluorobiphenyl)Cl_2 (**2d**; 200 mg, 0.245 mmol) in MeCN (2.0 mL) gave *cis*-[Au(P(*p*-OMe-C_6H_4)^tBu_2)(octafluorobiphenyl)(C_6F_5)(Cl)] (**3d**) as a white solid (94 mg, 45%). ^{1}H NMR (400 MHz, $CDCl_3$, 293 K, TMS): δ 7.69 (t, J = 9.0 Hz, 2 H), 7.21 (m, 1 H), 6.95 (dd, J = 8.8, 2.0 Hz, 2 H), 3.84 (s, 3 H), 1.56 (d, J = 15.2 Hz, 18 H). ^{19}F NMR (376 MHz, $CDCl_3$): δ −117.60 (m, 2 F), −123.68 (m, 2 F), −137.50 to −137.78 (m, 4 F), −138.46 (m, 1 F), −139.26 (m, 1 F), −156.81 (m, 1 F), −160.68 (m, 2 F). ^{31}P NMR (202 MHz, $CDCl_3$): δ 62.43 (s, 1 P). Anal. Calcd for $C_{33}H_{26}AuClF_{13}OP$: C, 41.77; H, 2.76. Found: C, 41.99; H, 2.86.

DOI: 10.1021/acs.organomet.7b00588
Organometallics XXXX, XXX, XXX−XXX

cis-[Au(P(p-Me-C$_6$H$_4$)^{t}Bu$_2$)(octafluorobiphenyl)(C$_6$F$_5$)(Cl)] (**3e**). The general procedure using AgF (56 mg, 0.44 mmol), TMSC$_6$F$_5$ (126 μL, 0.660 mmol), and *cis*-((*p*-Me-C$_6$H$_4$)^{t}Bu$_2$P)Au(octafluorobiphenyl)Cl$_2$ (**2e**; 200 mg, 0.250 mmol) in MeCN (2.0 mL) gave *cis*-[Au(P(*p*-Me-C$_6$H$_4$)^{t}Bu$_2$)(octafluorobiphenyl)(C$_6$F$_5$)(Cl)] (**3e**) as a white solid (158 mg, 68%). ^{1}H NMR (400 MHz, CDCl$_3$, 293 K, TMS): δ 7.63 (t, *J* = 8.0 Hz, 2 H), 7.23 (d, *J* = 8.0 Hz, 2 H), 7.21 (m, 1 H), 2.37 (s, 3 H), 1.58 (d, *J* = 16.0 Hz, 18 H). ^{19}F NMR (376 MHz, CDCl$_3$): δ −117.70 (m, 2 F), −123.64 (m, 2 F), −137.72 (m, 4 F), −138.42 (m, 1 F), −139.27 (m, 1 F), −156.81 (t, *J* = 19.3 Hz, 1 F), −160.69 (m, 2 F). ^{31}P NMR (202 MHz, CDCl$_3$): δ 62.29 (s, 1 P). Anal. Calcd for C$_{33}$H$_{26}$AuClF$_{13}$P: C, 42.49; H, 2.81. Found: C, 42.35; H, 3.09.

cis-[Au(PPh^{t}Bu$_2$)(octafluorobiphenyl)(C$_6$F$_5$)(Cl)] (**3f**). The general procedure using AgF (56 mg, 0.44 mmol), TMSC$_6$F$_5$ (126 μL, 0.660 mmol), and *cis*-(Ph^{t}Bu$_2$P)Au(octafluorobiphenyl)Cl$_2$ (**2f**; 180 mg, 0.229 mmol) in MeCN (2.0 mL) gave *cis*-[Au(PPh^{t}Bu$_2$)(octafluorobiphenyl)(C$_6$F$_5$)(Cl)] (**3f**) as a white solid (94 mg, 45%). ^{1}H NMR (400 MHz, CDCl$_3$, 293 K, TMS): δ 7.76 (t, *J* = 8.4 Hz, 2 H), 7.49−7.40 (m, 3 H), 7.20 (m, 1 H), 1.60 (d, *J* = 15.2 Hz, 18 H). ^{19}F NMR (376 MHz, CDCl$_3$): δ −117.76 (s, 2 F), −123.66 (m, 2 F), −137.62 to −137.79 (m, 4 F), −138.39 (m, 1 F), −138.89 (m, 1 F), −156.74 (m, 1 F), −160.50 (m, 2 F). ^{31}P NMR (162 MHz, CDCl$_3$): δ 62.59 (m, 1 P). Anal. Calcd for C$_{32}$H$_{24}$AuClF$_{13}$P: C, 41.83; H, 2.63. Found: C, 41.96; H, 2.81.

cis-[Au(P(p-Cl-C$_6$H$_4$)^{t}Bu$_2$)(Ar$_F$)(octafluorobiphenyl)(Cl)] (**3g**). The general procedure using AgF (56 mg, 0.44 mmol), TMSC$_6$F$_5$ (126 μL, 0.660 mmol), and *cis*-((*p*-Cl-C$_6$H$_4$)^{t}Bu$_2$P)Au(octafluorobiphenyl)Cl$_2$ (**2g**; 160 mg, 0.195 mmol) in MeCN (2.0 mL) gave *cis*-[Au(P(*p*-Cl-C$_6$H$_4$)^{t}Bu$_2$)(Ar$_F$)(octafluorobiphenyl)(Cl)] (**3g**) as a white solid (98 mg, 53%). ^{1}H NMR (400 MHz, CDCl$_3$, 293 K, TMS): δ 7.71 (t, *J* = 9.0 Hz, 2 H), 7.44 (d, *J* = 6.8 Hz, 2 H), 7.22 (m, 1 H), 1.55 (d, *J* = 15.6 Hz, 18 H). ^{19}F NMR (376 MHz, CDCl$_3$): δ −117.59 (m, 2 F), −123.75 (m, 2 F), −137.18 (m, 2 F), −137.68 (m, 2 F), −138.23 (m, 1 F), −139.01 (m, 1 F), −156.44 (m, 1 F), −160.51 (m, 2 F). ^{31}P NMR (202 MHz, CDCl$_3$): δ 62.86 (s, 1 P). Anal. Calcd for C$_{32}$H$_{23}$AuCl$_2$F$_{13}$P: C, 40.32; H, 2.43. Found: C, 40.02; H, 2.76.

cis-[Au(P(p-CF$_3$-C$_6$H$_4$)^{t}Bu$_2$)(octafluorobiphenyl)(C$_6$F$_5$)(Cl)] (**3h**). The general procedure using AgF (56 mg, 0.44 mmol), TMSC$_6$F$_5$ (126 μL, 0.660 mmol), and *cis*-((*p*-CF$_3$-C$_6$H$_4$)^{t}Bu$_2$P)Au(octafluorobiphenyl)Cl$_2$ (**2h**; 60 mg, 0.070 mmol) in MeCN (2.0 mL) gave *cis*-[Au(P(*p*-CF$_3$-C$_6$H$_4$)^{t}Bu$_2$)(octafluorobiphenyl)(C$_6$F$_5$)(Cl)] (**3h**) as a white solid (37 mg, 53%). ^{1}H NMR (400 MHz, CDCl$_3$, 293 K, TMS): δ 7.92 (t, *J* = 8.8 Hz, 2 H), 7.72 (d, *J* = 7.6 Hz, 2 H), 7.18 (m, 1 H), 1.55 (d, *J* = 16.0 Hz, 18 H). ^{19}F NMR (376 MHz, CDCl$_3$): δ −63.49 (s, 3 F), −117.57 (m, 2 F), −123.75 (m, 2 F), −136.99 (m, 2 F), −137.71 (m, 2 F), −138.25 (m, 1 F), −139.10 (m, 1 F), −156.25 (t, *J* = 19.9 Hz, 1 F), −160.41 (m, 2 F). ^{31}P NMR (202 MHz, CDCl$_3$): δ 64.09 (m, 1 P). Anal. Calcd for C$_{33}$H$_{23}$AuClF$_{16}$P: C, 40.16; H, 2.35. Found: C, 40.51; H, 2.68.

cis-(Ph^{t}Bu$_2$P)Au(octafluorobiphenyl)(p-HC$_6$F$_4$)Cl (**3i**). The general procedure using AgF (56 mg, 0.44 mmol), trimethyl(2,3,5,6-tetrafluorophenyl)silane (126 μL, 0.660 mmol), and *cis*-(Ph^{t}Bu$_2$P)Au(octafluorobiphenyl)Cl$_2$ (**2f**; 100 mg, 0.127 mmol) in MeCN (2.0 mL) gave *cis*-(Ph^{t}Bu$_2$P)Au(octafluorobiphenyl)(*p*-H-C$_6$F$_4$)Cl (**3i**) as a white solid (63 mg, 55%). ^{1}H NMR (400 MHz, CDCl$_3$, 293 K, TMS): δ 7.77 (t, *J* = 8.4 Hz, 2 H), 7.49−7.41 (m, 3 H), 7.22 (m, 1 H), 6.82 (m, 1 H), 1.59 (d, *J* = 15.2 Hz, 18 H). ^{19}F NMR (376 MHz, CDCl$_3$): δ −117.60 (m, 2 F), −125.27 (m, 2 F), −137.63 (m, 1 F), −137.82 (m, 3 F), −138.45 (m, 1 F), −138.66 (m, 2 F), −138.96 (m, 1 F), −160.51 (m, 2 F). ^{31}P NMR (202 MHz, CDCl$_3$): δ 62.32 (m, 1 P). Anal. Calcd for C$_{32}$H$_{25}$AuClF$_{12}$P: C, 42.66; H, 2.80. Found: C, 42.61; H, 3.17.

cis-(Ph^{t}Bu$_2$P)Au(octafluorobiphenyl)(p-CF$_3$C$_6$F$_4$)Cl (**3j**). The general procedure using using trimethyl(2,3,5,6-tetrafluoro-4-(trifluoromethyl)phenyl)silane (126 μL, 0.660 mmol), AgF (56 mg, 0.44 mmol), and *cis*-(Ph^{t}Bu$_2$P)Au(octafluorobiphenyl)Cl$_2$ (**2f**; 80 mg, 0.10 mmol) in 2.0 mL of MeCN gave *cis*-(Ph^{t}Bu$_2$P)Au(octafluorobiphenyl)(*p*-CF$_3$-C$_6$F$_4$)Cl (**3j**) as a white solid (66 mg, 67%). ^{1}H NMR (400 MHz, CDCl$_3$, 293 K, TMS): δ 7.76 (t, *J* = 9.2 Hz, 2 H), 7.50−7.41 (m, 3 H), 7.21 (m, 1 H), 1.61 (d, *J* = 15.2 Hz, 18 H). ^{19}F NMR (376 MHz, CDCl$_3$): δ −56.27 (t, *J* = 10.5 Hz, 3 F), −117.80 (m, 2 F), −122.23 (m, 2 F), −137.24 (m, 2 F), −137.54 (m, 1 F), −137.67 (m, 1 F), −138.28 (m, 1 F), −138.89 (m, 1 F), −140.08 (m, 2 F). ^{31}P NMR (202 MHz, CDCl$_3$): δ 62.40 (s, 1 P). Anal. Calcd for C$_{33}$H$_{24}$AuClF$_{15}$P: C, 40.91; H, 2.50. Found: C, 41.02; H, 2.93.

General Procedure for Preparation of Reductive Elimination Products from Biaryls: 2,2′,2″,3,3′,3″,4,5,5′,5″,6,6′,6″-Tridecafluoro-1,1′:4′,1″-terphenyl (4). In a glovebox, AgF (25 mg, 0.44 mmol), TMSC$_6$F$_5$ (62 mg, 0.26 mmol), and 2.0 mL of MeCN were placed in a 4 mL Schlenk tube that was equipped with a stirring bar. The reaction mixture was stirred in the dark for 3 h. (*t*Bu$_3$P)Au(octafluorobiphenyl)Cl$_2$ (100 mg, 0.130 mmol) was placed in the Schlenk tube, and the reaction mixture was stirred in the dark for 5 h. The solvent was removed, and the residue was purified by flash chromatography on silica gel (100%, *n*-pentane) to give 2,2′,2″,3,3′,3″,4,5,5′,5″,6,6′,6″-tridecafluoro-1,1′:4′,1″-terphenyl (**4**) as a white solid (43 mg, 71%). Mp: 144−145 °C. ^{1}H NMR (400 MHz, CDCl$_3$, 293 K, TMS): δ 7.31 (m, 1 H). ^{19}F NMR (376 MHz, CDCl$_3$): δ −136.81 (m, 2 F), −137.00 (m, 4 F), −137.28 (m, 2 F), −137.85 (m, 2 F), −149.38 (t, *J* = 20.9 Hz), −160.12 (m, 2 F) ppm. GC-MS (EI; *m*/*z*): 464. HRMS (EI; *m*/*z*): calcd for C$_{18}$HF$_{13}$: 463.9871; found: 463.9870. IR: ν 3080, 1507, 1244, 1136, 980, 953, 742, 722, 706 cm^{-1}.

2,2′,2″,3,3′,3″,5,5′,5″,6,6′,6″-Dodecafluoro-1,1′:4′,1″-terphenyl (**5**).[24] The general procedure using *cis*-(Ph^{t}Bu$_2$P)Au(octafluorobiphenyl)(*p*-HC$_6$F$_4$)Cl (**3i**; 100 mg, 0.111 mmol) in 2.0 mL of CDCl$_3$ gave 2,2′,2″,3,3′,3″,5,5′,5″,6,6′,6″-dodecafluoro-1,1′:4′,1″-terphenyl (**5**) as a white solid (42 mg, 85%). ^{1}H NMR (400 MHz, CDCl$_3$, 293 K, TMS): δ 7.30 (m, 2 H). ^{19}F NMR (376 MHz, CDCl$_3$): δ −137.08 (m, 4 F), −137.34 (m, 4 F), −137.82 (m, 4 F) ppm. GC-MS (EI; *m*/*z*): 464.

2,2′,2″,3,3′,3″,5,5′,5″,6,6′,6″-Dodecafluoro-4-(trifluoromethyl)-1,1′:4′,1″-terphenyl (**6**). The general procedure using *cis*-(Ph^{t}Bu$_2$P)Au(octafluorobiphenyl)(*p*-CF$_3$C$_6$F$_4$)Cl (**3j**; 100 mg, 0.103 mmol) in 2.0 mL of CDCl$_3$ gave 2,2′,2″,3,3′,3″,5,5′,5″,6,6′,6″-dodecafluoro-4-(trifluoromethyl)-1,1′:4′,1″-terphenyl (**6**) as a white solid (45 mg, 87%). Mp: 150−151 °C. ^{1}H NMR (400 MHz, CDCl$_3$, 293 K, TMS): δ 7.32 (m, 1 H). ^{19}F NMR (376 MHz, CDCl$_3$): δ −56.52 (t, *J* = 21.8 Hz, 3 F), −135.09 (m, 2 F), −136.26 (m, 2 F), −136.66 (m, 2 F), −137.18 (m, 2 F), −138.74 (m, 2 F) ppm. GC-MS (EI; *m*/*z*): 514; HRMS (EI; *m*/*z*): calcd for C$_{19}$HF$_{15}$, 513.9839; found, 513.9846. IR: ν 3087, 1657, 1480, 1342, 1256, 1150, 1002, 983, 726, 705 cm^{-1}.

Typical Procedure for Kinetic Study of C(sp^2)−C(sp^2) Reductive Elimination Reaction from Complex 3f. In an argon-filled glovebox, 0.02 mmol of complex **3f** was placed in a screw-cap NMR tube. CDCl$_3$ (0.4 mL) was used as the solvent, and trifluorotoluene or fluorobenzene was used as the internal standard. The NMR probe was heated at 85 °C. Thermolysis of complex **3f** was monitored by ^{19}F NMR spectroscopy. Kinetic data were fit to the expression $y = m_1 + m_2 \exp^{-t/K}$, in which $1/K$ is the first-order rate constant k_{obs}. All results were average of two runs.

Computational Methods. All of the DFT calculations were carried out with the Gaussian 09[25] series of programs. The B3LYP[26] functional with the standard 6-31G(d) basis set (SDD[27] for Au atoms) was used for geometry optimizations. The vibrational frequencies were computed at the same level of theory to determine whether the optimized structure was at an energy minimum or a transition state and to evaluate the corrections of enthalpy and Gibbs free energy. The B3LYP-D3[28] functional with the 6-311+G(d) basis set (SDD for Au atoms) was used to calculate the single-point energies. The solvent effects were considered by single-point calculations of the gas-phase stationary points with the SMD continuum model.[29] The energies reported in this paper are the B3LYP-D3 calculated Gibbs free energies in CDCl$_3$ on the basis of B3LYP calculated geometries with thermodynamic corrections calculated at the same level. In this study, the B3LYP functional, which has been verified to be a favorable functional for geometry optimization in a transition-metal-catalyzed system, was used for geometry optimization.[30] On the other hand, the addition of dispersion interaction into the B3LYP functional could describe the long-range interactions better, and thus an atom−atom

DOI: 10.1021/acs.organomet.7b00588
Organometallics XXXX, XXX, XXX−XXX

additive damped empirical potential of the form $-f(R)C^6/R^6$, which is named B3LYP-D3, was employed in our work to give more accurate energy information. This functional has also been widely used in Au and other transition-metal-catalyzed systems.[31] Consequently, the conclusion can be drawn that the B3LYP-D3 functional could provide accuracy in energetic information for this work. In general, the strain/electronic effects on a reaction mechanism could be addressed by a distortion/interaction model.[32] However, this model only could be applied on a bimolecular reaction system, which is for to this intramolecular reaction.

■ ASSOCIATED CONTENT

Supporting Information

The Supporting Information is available free of charge on the ACS Publications website at DOI: 10.1021/acs.organomet.7b00588.

Synthesis details, analytical data, NMR data of compounds **1a−i**, **2a−i**, **3a−j**, and **4−6**, X-ray diffraction data of complexes **3a−f,h−j** and *cis*-[Au(PPh_3)(Ar_F)Cl_2] (**2i**),[33] data for kinetic studies, and theoretical calculation of reductive elimination from complexes **3** (PDF)

Accession Codes

CCDC 1557972−1557981 contain the supplementary crystallographic data for this paper. These data can be obtained free of charge via www.ccdc.cam.ac.uk/data_request/cif, or by emailing data_request@ccdc.cam.ac.uk, or by contacting The Cambridge Crystallographic Data Centre, 12 Union Road, Cambridge CB2 1EZ, UK; fax: +44 1223 336033.

■ AUTHOR INFORMATION

Corresponding Authors

*E-mail for Y.L.: lanyu@cqu.edu.cn.

*E-mail for Q.S.: shenql@sioc.ac.cn.

ORCID

Yu Lan: 0000-0002-2328-0020

Qilong Shen: 0000-0001-5622-153X

Notes

The authors declare no competing financial interest.

■ ACKNOWLEDGMENTS

The authors gratefully acknowledge the financial support from the National Natural Science Foundation of China (21625206, 21632009, 21372247, 21572258, 21421002) and the Strategic Priority Research Program of the Chinese Academy of Sciences (XDB20000000).

■ REFERENCES

(1) (a) Hartwig, J. F. *Organotransition Metal Chemistry: From Bonding to Catalysis*; University Science Books: Sausalito, CA, 2009;. (b) Crabtree, R. H. *The Organometallic Chemistry of the Transition Metals*; Wiley: Hoboken, NJ, 2014.

(2) Reviews on carbon−carbon reductive elimination: (a) Brown, J. M.; Cooley, N. A. *Chem. Rev.* **1988**, *88*, 1031. (b) Yamamoto, A.; Yamamoto, T.; Ozawa, F. *Pure Appl. Chem.* **1985**, *57*, 1799.

(3) Reviews on carbon−heteroatom reductive elimination: (a) Hartwig, J. F. *Inorg. Chem.* **2007**, *46*, 1936. (b) Racowski, J. M.; Sanford, M. S. *Top. Organomet. Chem.* **2011**, *35*, 61. (c) Grushin, V. V. *Acc. Chem. Res.* **2010**, *43*, 160. (d) Desnoyer, A. N.; Love, J. A. *Chem. Soc. Rev.* **2017**, *46*, 197.

(4) Selected examples of $C(sp^2)-C(sp^2)$ reductive elimination from Ni(II) complexes: (a) Yamamoto, T.; Yamamoto, A.; Ikeda, S. *J. Am. Chem. Soc.* **1971**, *93*, 3350. (b) Komiya, S.; Abe, Y.; Yamamoto, A.; Yamamoto, T. *Organometallics* **1983**, *2*, 1466. (c) Coronas, J. M.; Muller, G.; Rocamora, M. *J. Organomet. Chem.* **1986**, *301*, 227. (d) Murakami, Y.; Yamamoto, T. *Inorg. Chem.* **1997**, *36*, 5682. (e) Yamamoto, T.; Abla, M.; Murakami, Y. *Bull. Chem. Soc. Jpn.* **2002**, *75*, 1997. (f) Yamamoto, T.; Yamaguchi, I.; Abla, M. *J. Organomet. Chem.* **2003**, *671*, 179. (g) Jin, L.-Q.; Zhang, H.; Li, P.; Sowa, J. R.; Lei, A.-W. *J. Am. Chem. Soc.* **2009**, *131*, 9892. (h) Xu, H.-W.; Diccianni, J. B.; Katigbak, J.; Hu, C.-H.; Zhang, Y.-K.; Diao, T.-N. *J. Am. Chem. Soc.* **2016**, *138*, 4779.

(5) Selected examples of $C(sp^2)-C(sp^2)$ reductive elimination from Pd(II) complexes: (a) Moravskiy, A.; Stille, J. K. *J. Am. Chem. Soc.* **1981**, *103*, 4182. (b) Deacon, G. B.; Gray, I. L. *Transition Met. Chem.* **1983**, *8*, 131. (c) Ozawa, F.; Yamamoto, T.; Yamamoto, A. *J. Organomet. Chem.* **1987**, *330*, 253. (d) Culkin, D. A.; Hartwig, J. F. *J. Am. Chem. Soc.* **2001**, *123*, 5816. (e) Culkin, D. A.; Hartwig, J. F. *Organometallics* **2004**, *23*, 3398. (f) Ananikov, V.; Musaev, D. G.; Morokuma, K. *Organometallics* **2005**, *24*, 715. (g) Osakada, K.; Onodera, H.; Nishihara, Y. *Organometallics* **2005**, *24*, 190. (h) Koizumi, T.; Yamasaki, A.; Yamamoto, T. *Dalton Trans.* **2008**, 3949. (i) Gensch, T.; Ronnefahrt, M.; Czerwonka, R.; Jager, A.; Kataeva, O.; Bauer, I.; Knolker, H. *Chem. - Eur. J.* **2012**, *18*, 770. (j) Klinkenberg, J. L.; Hartwig, J. F. *J. Am. Chem. Soc.* **2012**, *134*, 5758. (k) Gioria, E.; del Pozo, J.; Martinez-Ilarduya, J. M.; Espinet, P. *Angew. Chem., Int. Ed.* **2016**, *55*, 13276.

(6) Selected examples of $C(sp^2)-C(sp^2)$ reductive elimination from Pt(II) complexes: (a) Braterman, P. S.; Cross, R. J.; Young, G. B. *J. Chem. Soc., Dalton Trans.* **1977**, 1892. (b) Brune, H. A.; Stapp, B.; Schmidtberg, G. *J. Organomet. Chem.* **1986**, *307*, 129. (c) Himmel, S. E.; Young, G. B. *Organometallics* **1988**, *7*, 2440. (d) Merwin, R. K.; Schnable, R. C.; Koola, J. D.; Roddick, D. M. *Organometallics* **1992**, *11*, 2972. (e) Shekhar, S.; Hartwig, J. F. *J. Am. Chem. Soc.* **2004**, *126*, 13016. (f) Sugie, A.; Furukawa, H.; Suzaki, Y.; Osakada, K.; Akita, M.; Monguchi, D.; Mori, A. *Bull. Chem. Soc. Jpn.* **2009**, *82*, 555. (g) Robinson, R., Jr; Sharp, P. R. *Organometallics* **2010**, *29*, 1388. (h) Korenaga, T.; Abe, K.; Ko, A.; Maenishi, R.; Sakai, T. *Organometallics* **2010**, *29*, 4025. (i) Liberman-Martin, A. L.; Bergman, R. G.; Tilley, T. D. *J. Am. Chem. Soc.* **2013**, *135*, 9612. (j) Shiba, Y.; Inagaki, A.; Akita, M. *Organometallics* **2015**, *34*, 4844.

(7) Reviews about gold-catalyzed cross-coupling reactions: (a) Garcia, P.; Malacria, M.; Aubert, C.; Gandon, V.; Fensterbank, L. *ChemCatChem* **2010**, *2*, 493. (b) Wegner, H. A.; Auzias, M. *Angew. Chem., Int. Ed.* **2011**, *50*, 8236. (c) Hopkinson, M. N.; Gee, A. D.; Gouverneur, V. *Chem. - Eur. J.* **2011**, *17*, 8248. (d) de Haro, T.; Nevado, C. *Synthesis* **2011**, *2011*, 2530. (e) Boorman, T. C.; Larrosa, I. *Chem. Soc. Rev.* **2011**, *40*, 1910. (f) Miró, J.; del Pozo, C. *Chem. Rev.* **2016**, *116*, 11924. (g) Hopkinson, M. N.; Tlahuext-Aca, A.; Glorius, F. *Acc. Chem. Res.* **2016**, *49*, 2261.

(8) Selected examples of gold-catalyzed carbon−carbon bond-forming cross-coupling reactions: (a) Brenzovich, W. E., Jr.; Brazeau, J.-F.; Toste, F. D. *Org. Lett.* **2010**, *12*, 4728. (b) Hopkinson, M. N.; Tessier, A.; Salisbury, A.; Giuffredi, G. T.; Combettes, L. E.; Gee, A. D.; Gouverneur, V. *Chem. - Eur. J.* **2010**, *16*, 4739. (c) Qian, D.; Zhang, J. *Beilstein J. Org. Chem.* **2011**, *7*, 808. (d) Ball, L. T.; Lloyd-Jones, G. C.; Russell, C. A. *Science* **2012**, *337*, 1644. (e) Ball, L. T.; Lloyd-Jones, G. C.; Russell, C. A. *J. Am. Chem. Soc.* **2014**, *136*, 254. (f) Cambeiro, X. C.; Ahlsten, N.; Larrosa, I. *J. Am. Chem. Soc.* **2015**, *137*, 15636. (g) Hofer, M.; Genoux, A.; Kumar, R.; Nevado, C. *Angew. Chem., Int. Ed.* **2017**, *56*, 1021. (h) Cai, R.; Lu, M.; Aguilera, E. Y.; Xi, Y.-M.; Akhmedov, N. G.; Petersen, J. L.; Chen, H.; Shi, X.-D. *Angew. Chem., Int. Ed.* **2015**, *54*, 8772. (i) Patil, D. V.; Yun, H.; Shin, S. *Adv. Synth. Catal.* **2015**, *357*, 2622. (j) Hofer, M.; Genoux, A.; Kumar, R.; Nevado, C. *Angew. Chem., Int. Ed.* **2017**, *56*, 1021. (k) Xie, J.; Zhang, T.; Chen, F.; Mehrkens, N.; Rominger, F.; Rudolph, M.; Hashmi, A. S. K. *Angew. Chem., Int. Ed.* **2016**, *55*, 2934.

(9) (a) Tatsumi, K.; Hoffmann, R.; Yamamoto, A.; Stille, J. K. *Bull. Chem. Soc. Jpn.* **1981**, *54*, 1857. (b) Joost, M.; Amgoune, A.; Bourissou, D. *Angew. Chem., Int. Ed.* **2015**, *54*, 15022.

(10) (a) Tamaki, A.; Magennis, S. A.; Kochi, J. K. *J. Am. Chem. Soc.* **1974**, *96*, 6140. (b) Komiya, S.; Albright, T. A.; Hoffmann, R.; Kochi, J. K. *J. Am. Chem. Soc.* **1976**, *98*, 7255. (c) Komiya, S.; Kochi, J. K. *J.*

DOI: 10.1021/acs.organomet.7b00588
Organometallics XXXX, XXX, XXX−XXX

Am. Chem. Soc. **1976**, *98*, 7599. (d) Kuch, P. L.; Tobias, R. S. *J. Organomet. Chem.* **1976**, *122*, 429.
(11) (a) Vicente, J.; Bermudez, M. D.; Escribano, J. *Organometallics* **1991**, *10*, 3380. (b) Vicente, J.; Bermndez, M. D.; Carrion, F. J. *Inorg. Chim. Acta* **1994**, *220*, 1. (c) Hofer, M.; Gomez-Bengoa, E.; Nevado, C. *Organometallics* **2014**, *33*, 1328. (d) Wu, Q.; Du, C.-L.; Huang, Y.-M.; Liu, X.-Y.; Long, Z.; Song, F.-J.; You, J.-S. *Chem. Sci.* **2015**, *6*, 288. (e) Wolf, W. J.; Winston, M. S.; Toste, F. D. *Nat. Chem.* **2013**, *6*, 159. (f) Nijamudheen, A.; Karmakar, S.; Datta, A. *Chem. - Eur. J.* **2014**, *20*, 14650. (g) Joost, M.; Estevez, L.; Miqueu, K.; Amgoune, A.; Bourissou, D. *Angew. Chem., Int. Ed.* **2015**, *54*, 5236.
(12) Lavy, S.; Miller, J. J.; Pažický, M.; Rodrigues, A.; Rominger, F.; Jäkel, C.; Serra, D.; Vinokurov, N.; Limbach, M. *Adv. Synth. Catal.* **2010**, *352*, 2993.
(13) (a) Scott, V. J.; Labinger, J. A.; Bercaw, J. E. *Organometallics* **2010**, *29*, 4090. (b) Mankad, N. P.; Toste, F. D. *Chem. Sci.* **2012**, *3*, 72. (c) Mankad, N. P.; Toste, F. D. *J. Am. Chem. Soc.* **2010**, *132*, 12859. (d) Ghidiu, M. J.; Pistner, A. J.; Yap, G. P. A.; Lutterman, D. A.; Rosenthal, J. *Organometallics* **2013**, *32*, 5026. (e) Ghidiu, M. J.; Pistner, A. J.; Yap, G. P. A.; Lutterman, D. A.; Rosenthal, J. *Organometallics* **2013**, *32*, 6628. (f) Levin, M. D.; Toste, F. D. *Angew. Chem., Int. Ed.* **2014**, *53*, 6211. (g) Winston, M. S.; Wolf, W. J.; Toste, F. D. *J. Am. Chem. Soc.* **2015**, *137*, 7921. (h) Bhattacharjee, R.; Nijamudheen, A.; Datta, A. *Chem. - Eur. J.* **2017**, *23*, 4169. (i) Blaya, M.; Bautisa, D.; Gil-Rubiao, J.; Vincent, J. *Organometallics* **2014**, *33*, 6358.
(14) Corrie, T. J. A.; Ball, L. T.; Russell, C. A.; Lloyd-Jones, G. C. *J. Am. Chem. Soc.* **2017**, *139*, 245.
(15) Lu, P.-F.; Boorman, T. C.; Slawin, A. M. Z.; Larrosa, I. *J. Am. Chem. Soc.* **2010**, *132*, 5580.
(16) Hofer, M.; Nevado, C. *Tetrahedron* **2013**, *69*, 5751.
(17) (a) Tyrra, W.; Wickleder, M. S. *Z. Anorg. Allg. Chem.* **2002**, *628*, 1841. (b) Kremlev, M.; Mushta, A.; Tyrra, W.; Yagupolskii, Y.; Naumann, D.; Schafer, M. *Dalton Transactions* **2015**, *44*, 19693.
(18) For example, polar coordinating solvents enhanced the reductive elimination from a Pd(II) complex: Gillie, A.; Stille, J. K. *J. Am. Chem. Soc.* **1980**, *102*, 4933.
(19) Dolomanov, O. V.; Bourhis, L. J.; Gildea, R. J.; Howard, J. A. K.; Puschmann, H. *J. Appl. Crystallogr.* **2009**, *42*, 339.
(20) Sheldrick, G. M. *Acta Crystallogr., Sect. A: Found. Adv.* **2015**, *71*, 3.
(21) Sheldrick, G. M. *Acta Crystallogr., Sect. C: Struct. Chem.* **2015**, *71*, 3.
(22) Vicente, J.; Gonzalez-Herrero, P.; Garcia-Sanchez, Y. *Inorg. Chem.* **2004**, *43*, 7516.
(23) Hashmi, A. S. K.; Bechem, B.; Loos, A.; Hamzic, M.; Rominger, F.; Rabaa, H. *Aust. J. Chem.* **2014**, *67*, 481.
(24) Heidenhain, S. B.; Sakamoto, Y.; Suzuki, T.; Miura, A.; Fujikawa, H.; Mori, T.; Tokito, S.; Taga, Y. *J. Am. Chem. Soc.* **2000**, *122*, 10240.
(25) Frisch, M. J.; Trucks, G. W.; Schlegel, H. B.; Scuseria, G. E.; Robb, M. A.; Cheeseman, J. R.; Scalmani, G.; Barone, V.; Mennucci, B.; Petersson, G. A.; Nakatsuji, H.; Caricato, M.; Li, X.; Hratchian, H. P.; Izmaylov, A. F.; Bloino, J.; Zheng, G.; Sonnenberg, J. L.; Hada, M.; Ehara, M.; Toyota, K.; Fukuda, R.; Hasegawa, J.; Ishida, M.; Nakajima, T.; Honda, Y.; Kitao, O.; Nakai, H.; Vreven, T.; Montgomery, Jr., J. A.; Peralta, J. E.; Ogliaro, F.; Bearpark, M.; Heyd, J. J.; Brothers, E.; Kudin, K. N.; Staroverov, V. N.; Kobayashi, R.; Normand, J.; Raghavachari, K.; Rendell, A.; Burant, J. C.; Iyengar, S. S.; Tomasi, J.; Cossi, M.; Rega, N.; Millam, N. J.; Klene, M.; Knox, J. E.; Cross, J. B.; Bakken, V.; Adamo, C.; Jaramillo, J.; Gomperts, R.; Stratmann, R. E.; Yazyev, O.; Austin, A. J.; Cammi, R.; Pomelli, C.; Ochterski, J. W.; Martin, R. L.; Morokuma, K.; Zakrzewski, V. G.; Voth, G. A.; Salvador, P.; Dannenberg, J. J.; Dapprich, S.; Daniels, A. D.; Farkas, Ö.; Foresman, J. B.; Ortiz, J. V.; Cioslowski, J.; Fox, D. J. *Gaussian 09, Revision D.01*; Gaussian, Inc., Wallingford, CT, 2013.
(26) (a) Becke, A. D. *J. Chem. Phys.* **1993**, *98*, 5648. (b) Lee, C.; Yang, W.; Parr, R. G. *Phys. Rev. B: Condens. Matter Mater. Phys.* **1988**, *37*, 785.
(27) (a) Dolg, M.; Stoll, H.; Preuss, H. J. *J. Chem. Phys.* **1989**, *90*, 1730. (b) Dolg, M.; Wedig, U.; Stoll, H.; Preuss, H. *J. Chem. Phys.* **1987**, *86*, 866.
(28) Grimme, S.; Antony, J.; Ehrlich, S.; Krieg, H. *J. Chem. Phys.* **2010**, *132*, 154104.
(29) Marenich, A. V.; Cramer, C. J.; Truhlar, D. G. *J. Phys. Chem. B* **2009**, *113*, 6378.
(30) Sperger, T.; Sanhueza, I. A.; Kalvet, I.; Schoenebeck, F. *Chem. Rev.* **2015**, *115*, 9532.
(31) (a) Alcaide, B.; Almendros, P.; Cembellín, S.; Fernández, I.; Martínez del Campo, T. *Chem. Commun.* **2016**, *52*, 10265. (b) Jiang, J.; Liu, Y.; Hou, C.; Li, Y.; Luan, Z.; Zhao, C.; Ke, Z. *Org. Biomol. Chem.* **2016**, *14*, 3558. (c) Noey, E. L.; Luo, Y.; Zhang, L.; Houk, K. N. *J. Am. Chem. Soc.* **2012**, *134*, 1078. (d) Alcaide, B.; Almendros, P.; Fernández, I.; Martín-Montero, R.; Martínez-Peña, F.; Ruiz, M. P.; Torres, M. R. *ACS Catal.* **2015**, *5*, 4842. (e) Li, Y.; Qi, X.; Lei, Y.; Lan, Y. *RSC Adv.* **2015**, *5*, 49802.
(32) (a) van Zeist, W.; Bickelhaupt, F. M. *Org. Biomol. Chem.* **2010**, *8*, 3118. (b) Green, A. G.; Liu, P.; Merlic, C. A.; Houk, K. N. *J. Am. Chem. Soc.* **2014**, *136*, 4575. (c) Bhattacharjee, R.; Nijamudheen, A.; Karmakar, S.; Datta, A. *Inorg. Chem.* **2016**, *55*, 3023. (d) Bhattacharjee, R.; Nijamudheen, A.; Datta, A. *Org. Biomol. Chem.* **2015**, *13*, 7412. (e) Liu, S.; Lei, Y.; Qi, X.; Lan, Y. *J. Phys. Chem. A* **2014**, *118*, 2638. (f) Li, F.; Tu, Q.; Chen, S.; Zhu, L.; Lan, Y.; Gong, J.; Yang, Z. *Angew. Chem., Int. Ed.* **2017**, *56*, 5844.
(33) The X-ray crystal structure information is available at the Cambridge Crystallographic Data Centre (CCDC) under deposition numbers CCDC 1557972−1557981 for the compounds **2i** and **3a−f,h−j** reported in this article. These data can be obtained free of charge from The Cambridge Crystallographic Data Centre via www.ccdc.cam.ac.uk/data_request/cif or on application to the CCDC, 12 Union Road, Cambridge CB2 1 EZ, UK (fax: +44-1223/336-033; e-mail, deposit@ccdc.cam.ac.uk).

DOI: 10.1021/acs.organomet.7b00588
Organometallics XXXX, XXX, XXX−XXX